EFFECTS OF BLOOD CONTAMINATION ON CHEMICAL COMPOSITION AND ION RELEASING OF CALCIUM SILICATE-BASED MATERIALS

Miss Nareerat Thanavibul

A Thesis Submitted in Partial Fulfillment of the Requirements

for the Degree of Master of Science in Endodontology

Department of Operative Dentistry

FACULTY OF DENTISTRY

Chulalongkorn University

Academic Year 2018

ผลของการปนเปื้อนเลือดต่อองค์ประกอบทางเคมีและการปลดปล่อยไอออนของวัสดุประเภทแคลเซียมซิลิเกต

น.ส.นารีรัตน์ ธนวิบูลย์

วิทยานิพนธ์นี้เป็นส่วนหนึ่งของการศึกษาตามหลักสูตรปริญญาวิทยาศาสตรมหาบัณฑิต
สาขาวิชาวิทยาเอ็นโดดอนต์ ภาควิชาทันตกรรมหัตถการ
คณะทันตแพทยศาสตร์ จุฬาลงกรณ์มหาวิทยาลัย
ปีการศึกษา 2561

Thesis Title	EFFECTS OF BLOOD CONTAMINATION ON CHEMICAL COMPOSITION AND ION RELEASING OF CALCIUM SILICATE-BASED MATERIALS
By	Miss Nareerat Thanavibul
Field of Study	Endodontology
Thesis Advisor	Assistant Professor Chootima Ratisoontorn, Ph.D.

Accepted by the FACULTY OF DENTISTRY, Chulalongkorn University in Partial Fulfillment of the Requirement for the Master of Science

..... Dean of the FACULTY OF DENTISTRY

(Assistant Professor Suchit Poolthong, Ph.D.)

THESIS COMMITTEE

..... Chairman

(Assistant Professor Anchana Panichuttra, Ph.D.)

..... Advisor

(Assistant Professor Chootima Ratisoontorn, Ph.D.)

..... External Examiner

(Jaruma Sakdee, D.M.Sc)

นารีรัตน์ ธนวิบูลย์ : ผลของการปนเปื้อนเลือดต่อองค์ประกอบทางเคมีและการปลดปล่อยไอออนของวัสดุประเภทแคลเซียมซิลิเกต. (EFFECTS OF BLOOD CONTAMINATION ON CHEMICAL COMPOSITION AND ION RELEASING OF CALCIUM SILICATE-BASED MATERIALS) อ. ที่ปรึกษาวิทยานิพนธ์หลัก : ผศ. ทญ. ดร.ชุติมา ระติสุนทร

การศึกษามีวัตถุประสงค์เพื่อประเมินผลของการปนเปื้อนเลือดต่อองค์ประกอบทางเคมีและการปลดปล่อยไอออนของวัสดุประเภทแคลเซียมซิลิเกต โดยศึกษาในวัสดุประเภทแคลเซียมซิลิเกต ได้แก่ โปรรูทเอ็มทีเอ ไบโอเดนทีน และโทเทิลฟิลบีซีอาร์อาร์เอ็มพุตตี้ นำชิ้นงานตัวอย่างทำให้อยู่สภาวะปนเปื้อนเลือดและไม่ปนเปื้อนเลือด การศึกษาองค์ประกอบทางเคมีของชิ้นงานตัวอย่างโดยเครื่องวิเคราะห์การเลี้ยวเบนรังสีเอกซ์ร่วมกับกล้องจุลทรรศน์อิเล็คตรอนแบบส่องกราดที่ต่อกับชุดเอกซเรย์สเปคโตรสโคปีแบบกระจายพลังงานหลังจากนำชิ้นงานตัวอย่างแช่ในฟอสเฟสบัฟเฟอร์ซาไลน์เป็นเวลา 1, 7, 14 และ 28 วัน และศึกษาการปลดปล่อยไอออนของวัสดุจากน้ำที่แช่ชิ้นงานตัวอย่างโดยเครื่องวัดความเป็นกรดด่างและเครื่องอินดัคทีพลีคัพเพิลพลาสมา ออปติกเคิลอีมิสชั่นสเปคโทรมิเตอร์หลังจากนำชิ้นงานตัวอย่างแช่ในน้ำปราศจากไอออนเป็นเวลา 1, 7, 14 และ 28 วัน จากการศึกษาพบว่าเมื่อชิ้นงานตัวอย่างเกิดการปนเปื้อนเลือดพบการสร้างอะพาไทต์ช้ากว่า โดยโปรรูทเอ็มทีเอพบอะพาไทต์บนพื้นผิวของวัสดุเร็วที่สุดไม่ว่าจะอยู่ในสภาวะใด ไม่พบความแตกต่างอย่างมีนัยสำคัญจากการวัดความเป็นกรดด่างและการปลดปล่อยของแคลเซียมไอออนไม่ว่าชิ้นงานตัวอย่างจะอยู่ในสภาวะใด แต่หากชิ้นงานตัวอย่างเกิดการปนเปื้อนเลือดการปลดปล่อยของซิลิคอนไอออนจะลดลง จากการศึกษาครั้งนี้สรุปว่าหากวัสดุประเภทแคลเซียมซิลิเกตเกิดการปนเปื้อนเลือดจะส่งผลให้สร้างอะพาไทต์ช้าและปลดปล่อยซิลิคอนไอออนลดลงกว่าสภาวะที่ไม่เกิดการปนเปื้อนเลือด

ภาควิชา	ภาควิชาทันตกรรมหัตถการ	ลายมือชื่อนิสิต
		.....
สาขาวิชา	วิทยาเอ็นโดดอนต์	ลายมือชื่อ อ.ที่ปรึกษาวิทยานิพนธ์หลัก
		.....
ปี การศึกษา	2561	

5875816332 : MASTER OF SCIENCE
CALCIUM SILICATE-BASED MATERIALS, BLOOD CONTAMINATION, CHEMICAL COMPOSITION, ION RELEASE

Nareerat Thanavibul :

EFFECTS OF BLOOD CONTAMINATION ON CHEMICAL COMPOSITION AND ION RELEASING OF CALCIUM SILICATE-BASED MATERIALS.

ADVISOR: Asst. Prof. Chootima Ratisoontorn, Ph.D.

This study assessed the effects of blood contamination on the chemical composition and ion release of calcium silicate-based materials. ProRoot MTA (WMTA), Biodentine and TotalFill BC RRM putty (TRRM) were investigated. Materials were exposed to blood (blood-contaminated condition) or normal saline (non-blood-contaminated condition) for 24 hours. Three samples of each group were analysed for chemical composition using X-ray diffractometer and an energy-dispersive X-ray spectoscope with a scanning electron microscope after immersed in phosphate-buffered saline for 1, 7, 14 and 28 days. Five samples of each group were used to measure pH and ion release using a pH meter and inductively coupled plasma-optical emission spectrometer after immersed in deionized water for 1, 7, 14 and 28 days. Apatite formation was found in blood-contaminated groups later compared with non-blood-contaminated groups. In both conditions, WMTA demonstrated apatite formation earlier than the other materials. Silicon ion release was reduced in all blood-contaminated groups. Blood contamination delayed apatite formation and decreased silicon ion release on the surface of calcium silicate-based materials.

Department:	Department of Operative Dentistry	Student's Signature .....
Field of Study:	Endodontology	Advisor's Signature .....
Academic Year:	2018	

ACKNOWLEDGEMENTS

I would like to express my sincere thanks to many people. First of all, I would like to acknowledge my supervisor, Assistant Professor Dr. Chootima Ratisoontorn for her invaluable help and constant encouragement throughout the course of this thesis. I am most grateful for her teaching and advice, not only the research methodologies but also many other methodologies in life. I would not have achieved this far and this thesis would not have been completed without all the support that I have always received from her.

I would like to take this opportunity to thank all thesis committees, Assistant Professor Dr. Anchana Panichuttra and Dr. Jaruma Sakdee for thier valuable comments and suggestions.

This thesis was supported by many people included Assistant Professor Dr. Jerus Sucharitakul and Miss Supamas, at biochemistry division. I would like to thanks the officers of Oral Biology Research Center at faculty of dentistry and Scientific and Technological Research Equipment Center Chulalongkorn university for their valuable assistance and kindly help on supporting the laboratory instruments.

Special thanks are due to my family and friends, for thier continuous support and understanding, but also for solving when i had many problems throughout the period of this thesis.

This thesis has been written during my study at Endodontics dentistry, Department of operative dentistry, Chulalongkorn university which provide excellent working conditions.

In this project, financial issue was supported by the 90th anniversary of Chulalongkorn University Scholarship.

Nareerat Thanavibul

TABLE OF CONTENTS

Page

CONTENT OF FIGURES

Page

CONTENT OF TABLES

Page

CHAPTER I INTRODUCTION

Background and rationale

Recently, various materials have been developed for treatment of communications between the root canal and external surface (1). Immediate repair of a perforation with appropriate material is recommended for achieving the optimum outcome (1, 2). An ideal repair material would be non-toxic, insoluble in tissue fluids, dimensionally stable, antibacterial, radiopaque, easy to handle, hard tissue conductive, biocompatible and provide adequate seal (3).

Calcium silicate-based materials were introduced to endodontics in the 1990s. The potential advantages of these materials in endodontics are related to their physico-chemical and biological properties. Calcium silicate-based materials are biocompatible, non-toxic, non-shrinking, and usually chemically stable within the biological environment (4). A further advantage of these materials is their ability to form hydroxyapatite and ultimately create a bond between dentin and the material (5), and the reaction induced by its released substances may influence the outcome of treatment. Therefore, the bioactivity of materials plays a key role to promote healing.

Mineral trioxide aggregate (MTA) has these properties and can be differentiated from other root repair materials such as amalgam, super EBA and IRM by its additional

ability to conduct cementum and bone formation over its surface (6). A number of studies have demonstrated that MTA has excellent biocompatibility and sealing ability (7), which constitutes a basis for the wide range of applications of this material. The performance of MTA is largely attribute to its bioactivity. That is, the capacity to produce spontaneously an apatite layer when in contact with phosphate-containing physiological fluids (5, 8-12). The apatite formation is promoted via an interaction of calcium ion released from MTA with phosphates and considered as a basis for the biocompatibility of several inorganic biomaterials such as glass ceramics (13, 14). Moreover, MTA is also known to interact with dentine to cause intertubular calcium and silicon incorporation (15), intrafibrillar apatite deposition (10) and formation of a tag-like structure (5, 8, 15) in the presence of phosphate-buffered saline (PBS). Such a biomineralization ability may account for the sealing ability and dentine bonding of this material. Despite its many advantages, MTA also has some less than optimal properties, such as difficult to handle, long setting time (16, 17) and discoloration of teeth (18, 19).

To eliminate MTA's disadvantages, Biodentine was introduced. The powder consists of a tricalcium silicate cement, which is similar to the MTA and small proportions of dicalcium silicate, calcium carbonate and zirconium oxide are added as the radiopacifier (20). The liquid is composed of calcium chloride as an accelerator to reduce setting time and a hydrosoluble polymer (20). These materials is claimed to be used as a dentine restorative material in addition to endodontic indications similar to

those of MTA. Biodentine shows apatite formation after immersion in phosphate solution (21). This material is reported to induce pulp cell differentiation and biomineralization *in vitro*, suggesting its ability to stimulate reparative dentinogenesis after direct pulp capping (22, 23).

TotalFill Bioceramic Root Repair Material (TotalFill BC RRM) is another calcium silicate-based material. This material is composed of calcium silicate, zirconium oxide, tantalum oxide, calcium phosphate monobasic, and filler agents. It is produced in a premixed state as moldable putty and employs natural canal moisture in its setting reaction (24). The material is made of nanosphere particles. The fine particle size allows the materials to enter dentinal tubules and act with moisture inside the tubules for final setting as well as provide a mechanical seal (25, 26). Studies have reported TotalFill BC RRM, like white ProRoot MTA, showed bioactivity after placement in PBS. In a period of two months, all the materials tested showed a precipitation of apatite aggregate over the materials surfaces (27).

An ideal root repair material should not be affected by the contamination of physiologic solutions such as blood and/or saliva (28, 29). However, in view of its various applications, MTA may become contaminated by blood during placement. Torabinejad et al. (30) evaluated the effect of blood contamination on MTA in an *ex vivo* study by comparing the leakage of amalgam, Super EBA, IRM and the preliminary experimental prototype of MTA when applied to root-end cavities that were

contaminated by blood immediately after root resection. They reported that there was no significant difference between dye leakage in contaminated and uncontaminated groups and that MTA leaked significantly less than the other materials. In a laboratory bacterial leakage study, Montellano et al. (31) evaluated the effect of blood and/or saliva contamination on bacterial penetration of root-end cavities that were filled by tooth coloured MTA after root-end resection. Saliva-contaminated specimens demonstrated significantly more bacterial penetration than the uncontaminated group. However, blood contamination had no significant effect on bacterial penetration of root-end cavities that were filled by MTA. Conversely, Vanderweele et al. (32), when evaluating the retention characteristics of MTA in simulated furcation perforations, reported that in the blood contaminated group, MTA had significantly less resistance to displacement compared to the uncontaminated group at 7 days. Therefore, they recommended that blood should be removed before the placement of MTA. In contrast, Arens & Torabinejad (33) recommended that perforation sites should not be dried before the placement of MTA. In addition, Sluyk et al. (34) reported that the presence of moisture in a perforation site resulted in good adaptation of MTA to the perforation walls. Furthermore, they recommended a moistened matrix be positioned in the perforation defect before placement of MTA for ease of MTA condensation and to prevent over extrusion of the material. However, Al-Daafas & Al-Nazhan (35) found the use of an internal matrix beneath MTA, preventing its direct contact with the tissues, produced an adverse

healing response and reduced connective tissue attachment and bone formation in the site of the perforation.

Different calcium silicate-based materials may show varying degrees of bioactivity, because compositional differences may influence the ion releasing property of a material. In certain clinical applications, it could be difficult to completely avoid surface contaminated with blood and/or interstitial fluid. Therefore, the aim of this study was to evaluate the effect of whole blood exposure on chemical composition and ion releasing of three calcium silicate-based materials.

Objectives

The aim of the current study was to assess the effect of blood contamination on chemical composition and ion releasing of calcium silicate-based materials at days 1, 7, 14 and 28.

Scope of study

This *in vitro* study was carried out to assess in three calcium silicate-based materials that were exposed to blood or normal saline. Chemical compositions were analysed after each specimen was immersed in phosphate-buffered saline (PBS) for 1, 7, 14 and 28 days using X-ray diffractometer (XRD) and scanning electron microscope (SEM) with energy-dispersive X-ray spectroscopy (EDX). The pH value and ion release concentration were measured after each specimen was immermed in deionized water

for 1, 7, 14 and 28 days by Inductively coupled plasma optical emission spectrometer (ICP-OES).

CHAPTER II REVIEW RELATED LITERATURE

Root perforation

A root perforation is a mechanical or pathological communication formed between the supporting periodontal tissue of the tooth and the root canal system (36). Communication between the root canal system and supporting tissues of the tooth or oral cavity lowers the prognosis of endodontic treatment, and often leads to extraction of the tooth. An outcome study, showed that in retreatment cases only two factors significantly affected the success rate of the treatment, the presence of a preoperative radiolucency and the presence of a preoperative perforation (37).

The goal of perforation management is to maintain healthy periodontal tissues against the perforation without persistent inflammation or loss of periodontal attachment. In the case of periodontal tissue breakdown, the aim is to re-establish tissue attachment. Successful perforation repair depends on the ability to seal the perforation and to promote a healthy periodontal attachment of the repair material (38). The prognosis depends on the prevention or treatment of bacterial infection of the perforation site. In addition, the use of a non-irritating material which seals the perforation will limit inflammation. Several factors related to infection of the perforation site affect the prognosis of the treatment of root perforations, the most important of which are time between occurrence and treatment, size, and location of the perforation (Table 1) (2).

Table 1: Factors which affect prognosis of the treament of root perforations (2).

	Favorable	Questionable	Unfavorable
Time of repair	Immediate repair	Delayed repair	No repair or gross extrusion of the repair materials
Size	Small	Medium	Large
Location	Apical with no sulcular communication or osseous defect	Mid-root or furcal with no sulcular communication or osseous defect	Apical, crestal or furcal with sulcular communication and a probing defect with osseous destruction

Historically, many materials have been suggested for use in perforation repairs such as amalgam (39, 40), Cavit (39, 40), indium foil, zinc-oxide cements, ethoxybenzoic acid (Super EBA) (41), composites and glass ionomers (40, 42-44). Repair of perforations in the subcrestal region has been greatly facilitated in recent years by the development of a number of new materials.

Ideal characteristics of a perforation repair material (modified from Wang 2015) (45)

Various materials have been used to repair root perforations. The requirements for an ideal repair material have been described by several authors.

1. Physico-chemical properties

1.1 Short setting time

Setting time is the length of time for a material to transition from a fluid state into a hardened state. The presence of moisture is usually required for calcium silicate-based materials to set. A short setting time can help facilitate a tight seal between root canal system and periodontium, while a long setting time may result in difficulties with maintaining consistency of the mixture (46).

1.2 High mechanical strength

The compressive strength of a material is the value of uniaxial compressive stress reached when the material fails completely. It has been reported that high compressive strength of a root repair material could enable it to withstand loads tending to deformation and shrinkage (16).

1.3 High alkaline pH and calcium ion release

It has been suggested, by both *in vitro* and *in vivo* studies, the mechanism of pulp wound healing by the deposition of mineralized apatite depends on pH and the ability of calcium ion-release (47, 48).

1.4 High radiopacity, moderate flow, low porosity and solubility

Radiopacity is an essential physical property which allows the viewing of endodontic filling materials by radiographic examination, in order to check the obturation quality (16).

Flow is the ability of a cement to penetrate into the irregularities of the root canal system. However, if the flow is excessive, the risk of material extravasation to the periapical area is increased, which could damage periodontal tissues and compromise healing (49, 50). Thus, a moderate flow is preferred for the cement to access the areas that need to be filled.

Porosity is a common characteristic of materials as spaces between the material grains. The amount of porosity in mixed material is related to the amount of water (51), entrapment of air bubbles during the mixing procedure (52, 53), and the environmental acidic pH value (54).

Solubility is another factor in assessing the suitability of potential substances to be used as restorative materials in dentistry. Lack of solubility is a desired characteristic for root-end filling materials and materials used for perforation repair (16).

2. Biological properties

2.1 Biocompatibility

Materials used in endodontics are frequently placed in intimate contact with the pulp or periodontium and thus must be non-toxic and biocompatible with host tissues (45).

2.2 Stimulation of biomineralization

An optimal material used for perforation repair not only provides an effective seal, but also induces chemical bond formation and apatite precipitation in dentin over time (23). Biomineralization is likely to facilitate healing at the material-tissue interface, resulting in the elevation of local pH, the release of mineral ions and formation of apatite-like structures (5), so that the newly formed barrier of mineralized tissue can protect the root canal from bacteria and toxins.

Calcium silicate-based materials

Calcium silicate-based cements are cements or root canal sealers that have been made based on a composition of calcium and silicate. MTA is one of most popular calcium silicate-based materials used in endodontics because its posseses several of ideal properties such as good sealing ability and biocompatibility. Its clinical applications have broadened to include perforation repair, pulp capping, pulpotomy, and apexification. MTA requires the presence of water for setting. Therefore, set MTA can acquire its optimal strength and produce excellent sealing ability in the presence of

moisture (30). Researchers have been encouraged to investigate materials with similar favorable properties, while being less expensive as well as fewer drawbacks of the original MTA. Since 75% of MTA is composed of Portland cement (PC). Some investigators introduced their novel formulations as PC-based materials. These investigators claimed that their new materials had a similar composition to MTA with some modifications that may improve some of the properties such as handling characteristics, lower setting time, prevention of tooth discoloration, and higher radiopacity. Several materials, mostly composed of calcium and silicate (main components of PC) that are commercially available, such as Biodentine and TotalFill BC RRM

Mineral trioxide aggregation (MTA)

The original formulation of MTA was developed in the 1990s, and is manufactured by Dentsply International (Dentsply-Tulsa Dental, Johnson City, USA). MTA is a mixture of dicalcium silicate, tricalcium silicate, tricalcium aluminate, gypsum, tetracalcium aluminoferrite, and bismuth oxide. MTA was originally introduced in gray MTA (GMTA). Because of the discoloration potential of GMTA, white MTA (WMTA) was developed. Investigations showed that lower amounts of iron, aluminum, and magnesium were present in WMTA than in GMTA (55, 56). Bismuth oxide was used as radiopacifier of MTA (57).

When MTA powder is mixed with water, it undergoes two main reactions. Firstly, the tricalcium silicate and dicalcium silicate react with water to form calcium silicate hydrate and calcium hydroxide. Secondly, the tricalcium aluminate reacts with water, and in the presence of calcium sulfate initially produces ettringite (Table 2).

Table 2: Setting reaction of MTA (58)

$2(3CaO.SiO_2) + 6H_2O$ -->	$3CaO.2SiO_2.3H_2O + 3Ca(OH)_2$
tricalcium silicate + water	calcium silicate + calcium hydroxide
$2(2CaO.SiO_2) + 4H_2O$ -->	$3CaO.2SiO_2.3H_2O + Ca(OH)_2$
dicalcium silicate + water	calcium silicate + calcium hydroxide
$3CaO.Al_2O_3 + CaSO_4 + H_2O$ -->	$3CaO.Al_2O_3.3\ CaSO_4.31H_2O$
tricalcium aluminate + gypsum + water	ettringite

The ratio of calcium silicate drops because of the formation of a calcium precipitate. The precipitated calcium produces calcium hydroxide, which is the cause of MTA's high alkalinity after hydration (59).

Chemical and physiological properties

MTA is prepared by mixing the powder with sterile water in a 3:1 powder-to-liquid ratio (60). The mean setting time of MTA has been reported to be approximately 165 minutes, which is longer than amalgam, Super EBA and IRM (16, 61). MTA's long setting time is one of the major drawbacks of the material. Many investigations have been

performed to overcome this clinical disadvantage. Bortoluzzi et al. (62) evaluated the influence of addition of 10% calcium chloride ($CaCl_2$) on the setting time. The addition of $CaCl_2$ provided a significant reduction (50%) in the initial setting time of cements and the final setting time of WMTA was reduced in 35.5%.

There are many studies about MTA chemical composition after setting and various methods have been used to examine MTA composition including energy dispersive analysis with x-ray (EDAX), inductively coupled plasma optical emission spectroscopy (ICP-OES), x-ray diffraction analyses (XRD), x-ray fluorescence spectrometry (XRF), energy x-ray spectrometry, and energy dispersive spectroscopy (EDX). Several investigations have reported that the main elemental components of MTA are calcium and silica, as well as bismuth oxide (16, 17, 55, 56, 63).

The pH value of MTA is 10.2 after mixing and rises up to 12.5 after 3 hours (16). WMTA displays a significantly higher pH value 60 minutes after mixing compared to GMTA (64). MTA kept its high pH value throughout the course of a longterm study. The high pH value is attributed to the constant release of calcium ions from MTA and the formation of calcium hydroxide (65).

The release of calcium ions from MTA has been reported by several investigators (8, 9, 66). Despite the fact that the formation of apical barriers is highly successful using calcium hydroxide, this material is quickly resorbed when in contact with the apical tissues, making it necessary to follow the clinical case long-term to

confirm the formation of the barrier. Calcium release from MTA might be influenced by certain clinical conditions. Islam and associates found that the percent solubility of WMTA was greater than that of white Portland cement, ordinary Portland cement and GMTA (64). Solubility in this case may be beneficial to the success of the product in that it allows for the dissolution of components, which leads to the formation of reaction products at the interface between the material and the tooth, generating a biologic seal mostly of calcium hydroxide. The results of the degree of solubility of MTA have been contradictory between different studies (16, 64, 67, 68). However, increased solubility has been reported in a long-term study (69).

In various clinical applications, MTA encounters different physiological fluids as well as those introduced during endodontic procedures. Whether during setting or after setting, these solutions may impact the chemistry and properties of MTA. During setting, exposure of MTA to acidic environments, like those possible in inflamed pulpal or periapical tissues, will affect reaction product development. Lee et al. (70) observed a reduction of calcium hydroxide formation when MTA was exposed to a pH 5 solution. Furthermore, surface dissolution of reaction product particles was evident, leading to weakening of the material manifested as reduced microhardness. Exposure to serum has also been shown to detrimentally affect the setting of MTA as displayed by a difference in surface morphology and chemical distribution (71) as well as hardness (72, 73).

Biodentine

Biodentine (Septodont, Saint-Maur-des-Fosses, France) was introduced as a dentin replacement material in 2011. Biodentine contains tricalcium silicate, calcium carbonate, zirconium oxide, and a waterbased liquid-containing calcium chloride as the setting accelerator. Zirconium oxide is the radiopaque agent allowing identification on radiographs. According to the ISO 6876/2001, Biodentine displays a radiopacity greater than 3 mm thickness of aluminum (74).

Septodont claims to use a new technological platform named 'Active Biosilicate Technology™' to control the purity of the raw materials. Manufacturing pure synthetic tricalcium silicate instead of purifying the natural tricalcium silicate is advantageous as the mineral content is not changed by the sintering conditions or variations in the chemical composition of the raw materials (75). Moreover, synthetic tricalcium silicate does not contain heavy metals contrary to purified natural tricalcium silicate. This has been proved by the analysis of acid-extractable and leached of Biodentine which demonstrated absence of heavy element contamination (76). The use of pure synthetic tricalcium silicate instead of specific clinker has also been shown to result in enhanced material properties of Biodentine and MTA Angelus in comparison to MTA (75).

Setting reaction of Biodentine is hydration process, similar to others calcium silicate-based materials. The calcium silicate has the ability to interact with water leading to the setting and hardening of the cement. This is a hydration of the tricalcium silicate

(C3S; $3CaO.SiO_2$) which produces a hydrated calcium silicate gel (CSH gel) and calcium hydroxide ($Ca(OH)_2$) (Fig 1). This dissolution process occurs at the surface of each grain of calcium silicate. The hydrated calcium silicate gel and the excess of calcium hydroxide tend to precipitate at the surface of the particles and in the pores of the powder, due to saturation of the medium. This precipitation process is reinforced in systems with low water content.

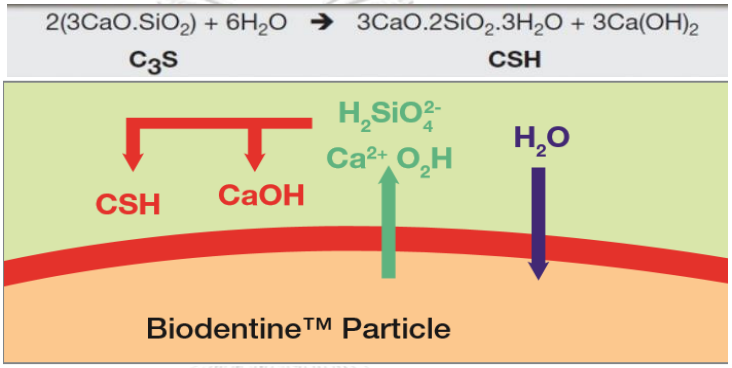

Figure 1: Setting reaction of Biodentine (77)

Chemical and physiological properties

According to the manufacturer's instructions, Biodentine is a fast-setting (around 10-12 minutes for initial setting) calcium silicate-based restorative material. The final setting time of Biodentine is assessed to be 45 minutes (74). An initial volume reduction due to chemical contraction and capillary absorption occurs during the first hours followed by a secondary expansion due to continuation of the hydration process.

Energy dispersive X-ray spectroscopy (EDX) analysis of set Biodentine confirmed elemental peaks for calcium, silicon, carbon, oxygen, zirconium and chlorine with

zirconium concentrated in specific areas while all other elements were equally distributed. X-ray diffraction (XRD) analysis exhibited definite peaks for calcium silicate, calcium carbonate, zirconium oxide and calcium hydroxide with a wavy base line indicating the presence of an amorphous compound. Fourier transform infrared spectroscopy (FT-IR) analysis of set Biodentine showed peaks at 3,400 (water or calcium hydroxide), 700 and 1,420 cm-1 (calcium carbonate) and an Si–O absorption band at 960 cm-1 referring to calcium silicate hydrate (78).

The pH of the leachate, when set Biodentine was stored in deionized water, was recorded as 9.14 ± 0.16, 8.88 ± 0.27 and 8.02 ± 0.19 at 3 hours, 1 day and 1 week, respectively (79). In another study where the pH of the medium in HBSS was measured, the pH was recorded as 11.7, 12.1, 12.3, 12.4 and 12.3 at 1, 7, 14, 21 and 28 days, respectively, confirming the alkalinity of the cement. The pH of BiodentineTM is similar to that of Bioaggregate and IRM (80).

Comparing calcium release of Biodentine with other bioceramic materials, Biodentine showed a higher level of calcium ion release than MTA, EndoSequence BC Sealer (BC Sealer), BioAggregate, TCS-Zr, and intermediate restorative material (IRM) (80, 81). The incorporation of calcium and silicate was detected deep in Biodentine-treated root dentin after immersion in phosphate-buffered saline (PBS) for 90 days (81). Moreover, Grech et al. (74) demonstrated negative solubility values for a prototype cement, Bioaggregate and Biodentine, in a study assessing the physical properties

ofthe materials. They attributed this result to the deposition of substances such as hydroxyapatite on the material surface when in contact with synthetic tissue fluids.This property is rather favorable as they indicate that the material does not lose particulate matter to result in dimensional instability.

TotalFill BC Root Repair Material (TotalFill BC RRM)

TotalFill BC RRM (FKG, La Chaux-de-Fonds, Switzerland) is another bioceramic material that has been developed recently. According to the manufacturer, TotalFill BC RRM is composed of calcium silicates, zirconium oxide, tantalum oxide, calcium phosphate monobasic and filler agents. It is produced as a premixed product in mouldable putty to provide the clinician with a homogeneous and consistent material that sets in the presence of moisture.

Chemical and physiological properties

According to the manufacturer TotalFill BC RRM has a working time of more than 30 minutes and approximately a 4-hour setting time. Presence of moisture is required for the material to harden. The fine particle size allows the material to enter dentinal tubules and act with moisture inside the tubules for final setting as well as provide a mechanical seal (26).

The pH value of TotalFill BC RRM has been reported be as high as 12.4, which is probably responsible for its antibacterial properties during the setting reaction. Hansen et al. (82) compared the pH changes in simulated root resorption defects filled with MTA

and TotalFill BC RRM, and concluded that intracanal placement of MTA resulted in a higher pH than TotalFill BC RRM. The pH value of both TotalFill BC RRM and MTA treated canals declined to the levels of the negative control after a 4-week incubation in saline.

Ma et al. (3) used EDX to confirm the chemical composition of the two materials; the results revealed that TotalFill BC RRM putty and paste crystals have similar elements (calcium, silicate, phosphate, carbon and oxygen) but different overall composition to GMTA (tricalcium silicate, dicalcium silicate, bismuth oxide, and small proportions of tricalcium aluminate and calcium sulfate). Moreover, TotalFill BC RRM putty and paste each have a similar crystallographic surface structure to GMTA, showing hexagonal-shaped crystals varying in size, appearing both discretely and in aggregates (3). Another recent study analyzed the structure and composition variations of TotalFill BC RRM over a longer period of time (27). Results showed the precipitation of apatite and an increase of calcium and phosphate on the surface of the material after a 2-month immersion in PBS.

Effects of blood contamination on calcium silicate-based materials

Calcium silicate-based materials is considered as the material of choice in vital pulp therapies, for the repair of accidental and/or pathological root perforations, as an apical root canal plug in immature teeth with necrotic pulp tissue and as a root-end

filling material in endodontic surgery. In all of these clinical situations, MTA comes into contact with blood and tissue fluid.

An ideal root repair material should not be affected by the contamination of physiological solutions such as blood and/or saliva (28, 29). However, in view of its various applications, MTA may become contaminated by blood during placement. Torabinejad et al. (30) evaluated the effect of blood contamination on MTA in an ex vivo study by comparing the leakage of amalgam, Super EBA, IRM and the preliminary experimental prototype of MTA when applied to root-end cavities that were contaminated by blood immediately after root resection. They reported that there was no significant difference between dye leakage in contaminated and uncontaminated groups and that MTA leaked significantly less than the other materials.

In a laboratory bacterial leakage study, Montellano et al. (31) evaluated the effect of blood and/or saliva contamination on bacterial penetration of root-end cavities that were filled by tooth coloured MTA after root-end resection. Saliva-contaminated specimens demonstrated significantly more bacterial penetration than the uncontaminated group. However, blood contamination had no significant effect on bacterial penetration of root-end cavities that were filled by MTA.

Conversely, when evaluating the retention characteristics of MTA in simulated furcation perforations, reported that in the blood contaminated group, MTA had significantly less resistance to displacement compared to the uncontaminated group at

7 days (32). Therefore, they recommended that blood should be removed before the placement of MTA. In contrast, Arens and Torabinejad (33) recommended that perforation sites should not be dried before the placement of MTA. In addition, Sluyk et al. (34) reported that the presence of moisture in a perforation site resulted in good adaptation of MTA to the perforation walls. Furthermore, they recommended a moistened matrix be positioned in the perforation defect before placement of MTA for ease of MTA condensation and to prevent over-extrusion of the material. However, Al-Daafas and Al-Nazhan (35) found the use of an internal matrix beneath MTA, preventing its direct contact with the tissues, produced an adverse healing response and reduced connective tissue attachment and bone formation in the site of the perforation.

The absence of the acicular crystals was also reported as a result of exposure of MTA specimens to blood contaminated. Spot analysis of the acicular crystals by EDX indicated that they were rich in sulphur and aluminium as compared to the background matrix, suggestive of ettringite crystals (20). Lee et al. (70), Kayahan et al. (83) and Nekoofar et al. (84, 85) associated the lack of acicular crystals with the reductions in compressive strength and surface microhardness of acid and blood-contaminated MTA.

Jasiczak and Zielinski (52) demonstrated the air entrainment effect of red blood cells when mixed with Portland cement. Remadnia et al. (86) revealed that haemoglobin or whole animal blood when used as an admixture to portland cement resulted in the increased porosity of the material, which is in accordance with the results of Nekoofar et

al. (20). Formation of microchannels and interconnected pore networks is key for the full formation of crystalline phases (87) and the progression of hydration (51).

Charland et al. (88) evaluated the abilities of MTA and ESRRM to set in the presence of human blood. The setting times for both materials in this study were much longer than those reported by the respective manufacturers. All samples of MTA were set by 36 hours, whereas the ESRRM samples were not completely set by 48 hours. Accordingly, Alhodiry et al. (89) tested the effect of contamination with fresh blood on the setting time of MTA and Biodentine. The mean setting time of Biodentine and MTA for the blood-contaminated samples were 46 and 114 minutes respectively. The results showed that the setting time was significantly different and prolonged for both Portland cement and Biodentine when contaminants were added.

Therefore, there is a basis for the recommendation that clinicians should attempt to control bleeding when placing MTA in any clinical situation. Interestingly, white MTA had greater hardness than gray MTA irrespective of the level of blood contamination. However, quite unexpectedly, white MTA mixed with blood had a greater hardness than white MTA only exposed to blood, and was harder than all other experimental groups. The reason for this difference is unclear, and further investigation is warranted. If contamination with blood is unavoidable, white MTA may be a preferred choice over gray MTA. The same study also found that the surface microhardness values of MTA after 6 months were similar to those after 4 days (85).

Bioactivity

Bioactivity is the ability of a biomaterial to induce a specific biological response. One of the characteristics of MTA is its ability to form a hydroxyapatite(8) or apatite-like layer(10) on its surface when it comes in contact with phosphate containing fluids, a phenomenon called biomineralization. The ISO 23317 method is used to evaluate layers precipitated on the materials. Molds are filled with prepared cements. SEM with EDX provides qualitative and semi-quantitative measurements of atomic calcium and phosphorous to calculate the superficial calcium to phosphorus atomic (Ca/P) ratios (90, 91). The mechanism of apatite formation on calcium silicate MTA cements in phosphate-containing solutions was summarized by Gandolfi et al. (11) in 11 steps. The growth of a layer of apatite is an ideal environment for stem cell and osteoblast differentiation and colonization to support new bone formation (92). The presence of an extensive spatite layer on materials promotes the adsorption of proteins and the formation of a protein layer that favours osteoblast adhesion (93, 94). Apatite together with the epigenetic signals correlated to ion release may well explain the excellent clinical outcomes of MTA cements (95). Moreover, the ability to form apatite may provide clinical advantages by improving their sealing by the deposition of calcium phosphates.

Apatite formation

The apatite forming ability of a material in the presence of phosphate-containing solutions is achieving bonds between the material and bone (96). Various calcium

silicate-based materials are reported to show this ability (75, 97). The formation of apatite layer on the calcium silicate-based materials occured following chemical reactions between products from materials and solutions (figure 2). Ion exchange occurs following hydration of calcium silicate particles and form calcium silicate hydrate and calcium hydroxide, that creates an alkaline environment. Although these reactions occur almost immediately after cement hydration and continuous release of calcium and silicon ions after initial setting. Calcium carbonate is formed from the surface carbonation of cements by reaction of the calcium hydroxide with the carbon dioxide in environment. Cation exchange increases the hydroxyl concentration of the solution. The surfaces of the calcium silicate particles are attack by hydroxyl ions in solution, resulting in hydrolysis of SiO^{4-} group in an alkaline environment. The result is the formation of an amorphous calcium silicate hydrate phase. Calcium silicate hydrate containing silanol (Si-OH) groups, which negative charges surface occur (SiO^{-}; deprotonation of silanol groups at alkaline pH) and interaction with calcium ions, resulting in an increase of cations on the set cement surface that may act as nucleation sites for apatite formation (96). When the set calcium silicate cement is immersed in phosphate-containing solutions, interaction between calcium from the cement and phosphate from the solution, which results in the formation of an amorphous calcium phosphate phase at nucleation site. The amorphous calcium phosphate undergoes phase transformation over time into apatite.

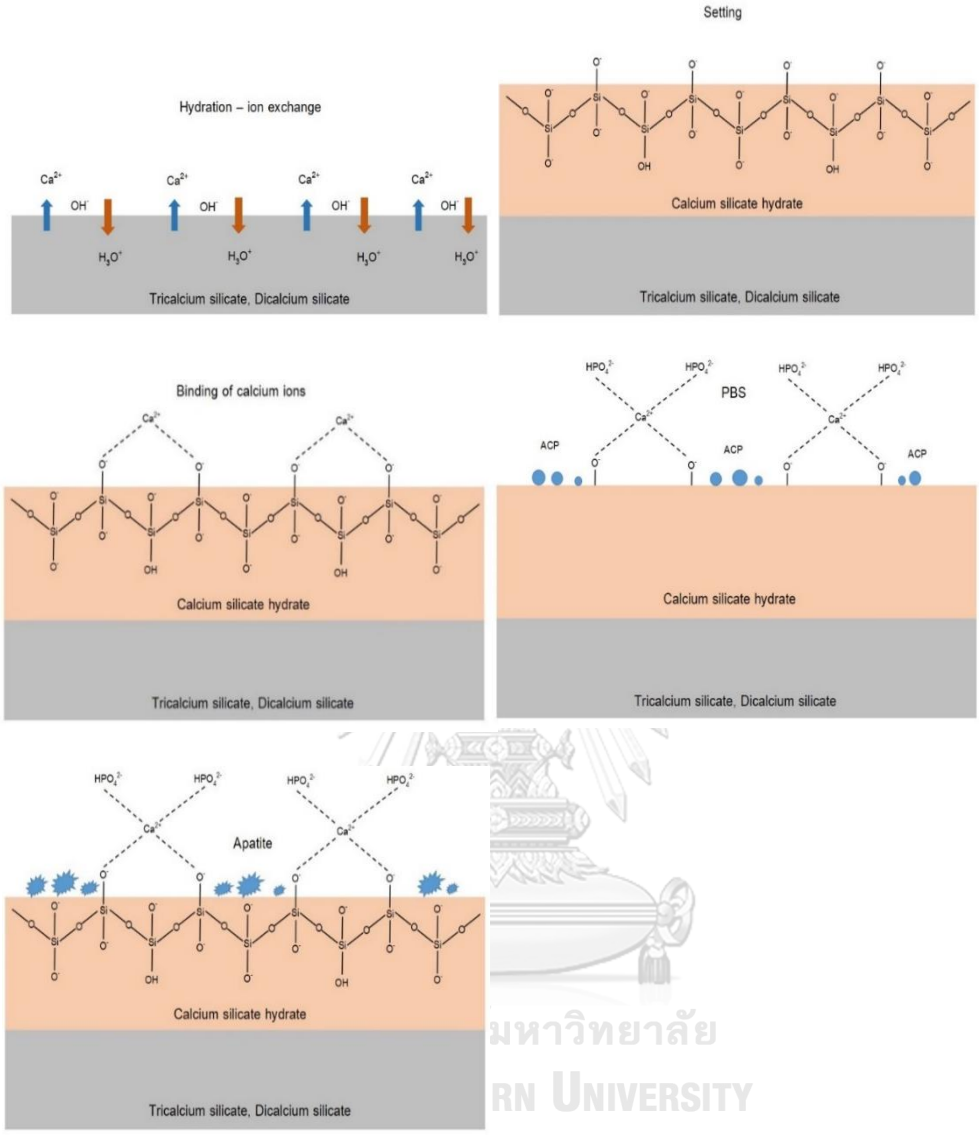

Figure 2: Apatite formation

pH and Ion releasing

It has been suggested, by both *in vitro* and *in vivo* studies, that the mechanism of pulp wound healing by the deposition of mineralized apatite depends on pH and the ability of calcium ion-release (47, 98). Moisture facilitates the hydration reactions of calcium silicates to produce calcium silicate hydrogel and calcium hydroxide, which

partially react with the phosphate to form hydroxyapatite and water (99, 100). Despite the fact that the formation of apical barriers is highly successful using calcium hydroxide, this material is quickly resorbed when in contact with the apical tissues, making it necessary to follow the clinical case long-term to confirm the formation of the barrier. MTA offers a barrier with excellent sealing properties and a high degree of biocompatibility (101).

X-ray diffractometer (XRD)

XRD analysis identifies the crystalline phases of cements, but not amorphous structures. The principle of XRD analysis is to compare the experimental pattern with a pattern simulated based on the presumed amounts, crystal parameters and equipment parameters of a mixture of known phases. The XRD is used to semi-quantitatively identify and quantify the main phases related to the MTA hydration process: tricalcium silicate, dicalcium silicate, calcium hydroxide, ettringite, bismuth oxide, and tricalcium aluminate. Tricalcium silicate and dicalcium silicate, that is, the main crystalline phases involved in the hydration of MTA (59, 63, 64, 102), were detected in the XRD analysis. Diffraction patterns provide information on the chemical characterization of cements, which is relevant to the understanding of the material's performance (59). One disadvantage of XRD is that it may not accurately identify some compounds with ingredients in quantities of less than 5% (64). Phase compositions of MTA specimens from each group are determined using an x-ray diffractometer and CuKa radiation. To

identify crystalline compounds, all patterns are matched using the database of the International Centre for Diffraction Data. The Rietveld refinement tool is used for the quantitative analysis of phases. It has already been reported that tricalcium silicate is one of the main phases present in unhydrated cements, accounting for a large portion of the MTA (59, 64, 102) and Portland cement powder (59, 63, 103). The percentage of calcium silicate will depend on the type of cement and on the manufacturing process (104). Although a large proportion of calcium silicate in relation to other phases was observed in the powders (59, 102), the real percentage of the compound was not calculated due to the presence of several uncharacterized peaks resulting from an amorphous phase or a combination of phases with low crystallinity. The use of internal reference patterns in the XRD analysis would allow the identification and quantification of amorphous phases (59).

Scanning electron microscope (SEM) and Energy-dispersive X-ray spectroscopy (EDX)

Scanning electron microscope (SEM), accompanied by x-ray analysis, is considered a relatively rapid, inexpensive and basically nondestructive approach to surface analysis It is often used to survey surface analytical problems before proceeding to techniques that are more surface sensitive and specialized. Energy-dispersive X-ray spectroscopy (EDX) is an analytical technique that qualitatively and quantitatively identifies the elemental composition of materials analyzed in an SEM,

which generally analyzes the top two microns of the sample with a spatial resolution of one micron. EDX analysis is used to identify essential compounds of the bioceramic cements, such as calcium, aluminum, bismuth, silicon, and sulfur.

An SEM is a powerful tool for microstructural evaluation of dental materials. In the SEM technique, an electron beam scans the surface of the sample to produce a variety of signals, the characteristics of which depend on many factors including the energy of an electron beam and the nature of the sample. Three types of signals provide the greatest amount of information in SEM: the secondary electrons (SE), back-scattered electrons (BSE), and x-rays (105). SE are emitted from the atoms on the surface, which produce a readily interpreted image, the contrast of which is determined by the sample morphology. The small diameter of the primary electron beam helps in obtaining a high resolution image. Back-scattered electrons are primary beam electrons that are reflected from atoms. The atomic number of the sample elements determines the image contrast of a back-scattered micrograph (106). Therefore, the image obtained with the back-scattered mode will show the distribution of different chemical phases in a sample. However, the resolution in such an image is not as good as that obtained through the secondary electrons due to the emission of electrons from different depths in the sample (107).

The hydration dynamics and mechanisms of bioceramic materials can be analyzed by several different methods including microscopy, elemental analysis, and

phase analysis (59, 75, 103, 108). The x-ray diffractogram identifies crystalline and particular phases in the materials. SEM is well suited for the study of material surface microstructures. EDX analysis allows qualitative analysis of the various elements on the surface layers of the materials. According to Camilleri et al. (75) these techniques are an adjunct to phase analysis by XRD and aid to verify the phases identified where peak overlap exists which is the main disadvantage with the use of XRD to analyze cement based materials. To overcome this problem, a method developed by Rietveld et al. (109) can be employed. In this method, powder diffraction analysis is standardized using calculated reference diffraction patterns that are based on models of crystal structures (110).

Inductively Coupled Plasma – Optical Emission Spectrometer (ICP-OES)

Inductively Coupled Plasma – Optical Emission Spectrometer (ICP-OES) is an analytical technique used for elemental determinations. The sample is subjected to temperatures high enough to cause not only dissociation into atoms but to cause signigicant amounts of collisional excitation of the sample atoms to take place. Once the atoms or ions are in thier excited states, they can decay to lower states through thermal or radiative (emission) energy transitions. In OES, the intensity of the light emitted at specific wavelengths is measured and used to determine the concentrations of the elements of interest.

One of the most important advantages of OES results from the excitation properties of the high temperature sources used in OES. These thermal excitation sources can populate a large number of different energy levels for several different elements at the same time. All of the excited atoms and ions can then emit their characteristic radiation at nearly the same time. This results in the flexibility to choose from several different emission wavelengths for an element and in the ability to measure emission from several different elements concurrently. However, a disadvantage associated with this feature is that as the number of emission wavelengths increases, the probability also increases for interferences that may arise from emission lines that are too close in wavelength to be measured seperately (111).

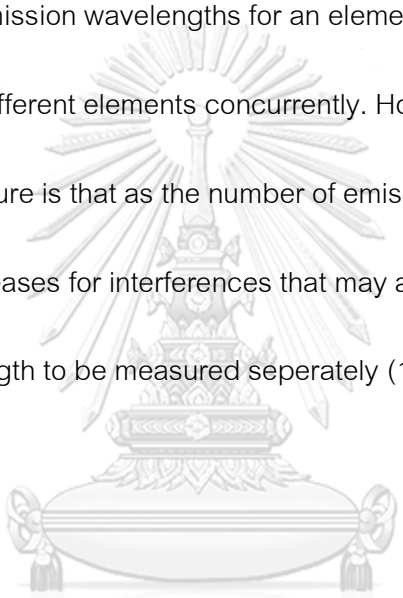

CHAPTER III RESEARCH METHODOLOGY

Target Population

Calcium silicate-based materials

Sample

WMTA, Biodentine, TRRM

Independent Variables

Blood contamination

Material

Time observed

Dependent Variables

Time of apatite formation

Calcium to phosphorus atomic ratio

Concentration of calcium, silicon and phosphorus ions

Control variables

Volume of blood and normal saline, size of the materials, amount of phosphate buffered solution and deionized water

Confounding Factors

Human error from mold preparation and removal of samples from mold

Hypothesis

Hypothesis I

H_0; There is no difference in chemical composition of three calcium silicate-based materials between the presence and absence of blood.

H_1; There is at least one difference from the others in chemical composition among three calcium silicate-based materials between the presence and absence of blood.

Hypothesis II

H_0; There is no difference in ion releasing of three calcium silicate-based materials between the presence and absence of blood.

H_1; There is at least one difference from the others in ion releasing among three calcium silicate-based materials between the presence and absence of blood.

Ethical Consideration

Ethical issue was approved by Research Ethics Committee of Faculty of Dentistry, Chulalongkorn University (HREC-DCU 2017-051) because of using human blood.

Materials

1. ProRoot MTA (WMTA; Dentsply Maillefer, Tulsa, OK, USA)

2. Biodentine (Septodont, Saint Maur des Fossés, France)

3. TotalFill BC RRM (TRRM; BUSA, BRASSELER, Savannah, GA, USA)

4. Plaster of Paris

5. 20-mm diameter, 2-mm height PVC ring

6. Incubator

7. Phosphate buffered solution (PBS)

8. Deionized water

9. Vacuum desiccator

10. UV light chamber

11. X-ray diffractometer (XRD; D8 Discover, Bruker, Karlsruhe, Germany)

12. Scanning Electron Microscope (SEM; JSM-6610LV, JEOL, Tokyo, Japan) and Energy Dispersive X-Ray Spectrometer (X-Max^{N} 50, Oxford instruments, Oxfordshire, United Kingdom)

13. 15 ml centrifuge tube

14. Micropipette

15. Human blood

16. Normal saline solution

Methods

Three calcium silicate-based materials, ProRoot MTA (WMTA; Dentsply Maillefer, Tulsa, OK, USA), Biodentine (Septodont, Saint Maur des Fossés, France) and TotalFill BC RRM (TRRM; BUSA, BRASSELER, Savannah, GA, USA) were evaluated. The compositions and manufacturers of the test materials are given in Table 3.

Table 3: Composition of test materials

Material		Composition	Manufacturer
ProRoot MTA	Powder Liquid	Tricalcium silicate, dicalcium silicate, tricalcium aluminate, bismuth oxide, calcium sulphate Water	Dentsply Maillefer, Tulsa, OK, USA
Biodentine	Powder Liquid	Tricalcium silicate, dicalcium silicate, calcium carbonate, iron oxide, zirconium oxide Water, calcium chloride, water reducing agent	Septodont, Saint Maur des Fossés, France
TotalFill BC RRM		Tricalcium silicate, dicalcium silicate, calcium phosphate monobasic, calcium hydroxide, colloidal silica, water-free thickening agent	FKG, La Chaux-de-Fonds, Switzerland

Sample preparation

WMTA was mixed according to the manufacturer's instructions at a 3:1 powder-to-water ratio. Biodentine was mixed according to the manufacturer's instructions by pouring 5 drops from the single-dose container into the capsule, close the capsule, place the capsule on an amalgamator at a speed of 4,000 rotations/minute and mix for 30 seconds. TotalFill BC RRM was a premixed material with putty consistency.

Whole fresh human blood was collected from a healthy consented volunteer 20 cc by a medical laboratory technologist in accordance with with the Human Research Ethics Committee of the Faculty of Dentistry, Chulalongkorn University (HREC-DCU 2017-051).

Plaster of Paris molds (internal dimensions 5 mm and thickness 2 mm) which first stored at 37 ± 1°C in a water bath for 24 hours.

Molds were placed on a glass slide. Each mould had been pre-filled with 10 µl of whole fresh blood that was then gently aspirated (Figure 3). Therefore, the internal surface of the mold was filled with blood prior to place test material. In groups without blood contamination, normal saline solution was used instead of blood. Six experimental groups were divided as follows.

Group 1: WMTA mixed with distilled water without blood contamination (WMTA/non-blood)

Group 2: WMTA mixed with distilled water with blood contamination (WMTA/blood)

Group 3: Biodentine without blood contamination (Biodentine/non-blood)

Group 4: Biodentine with blood contamination (Biodentine/blood)

Group 5: TotalFill BC RRM without blood contamination (TRRM/non-blood)

Group 6: TotalFill BC RRM with blood contamination (TRRM/blood)

Each material was placed in the mold (Figure 4). Specimens were stored in an incubator for 1 day (37 ± 1°C, >95% relative humidity). After setting (Figure 5), all samples were sterilized by ultraviolet light for 30 min per side according to the methods of Guerreiro-Tanomaru et al.(2013) (112).

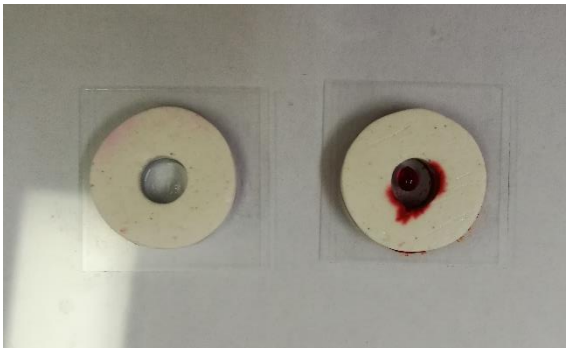

Figure 3: Each mold had been pre-filled with normal saline or whole fresh blood.

Figure 4: Each material was placed in the mold.

Figure 5: After setting of samples.

Chemical composition analysis

After setting, specimens were immersed individually in plastic centrifuge containing 5 ml. of PBS (136.4 mmol L^{-1} NaCl, 2.7 mmol L^{-1} KCl, 8.2 mmol L^{-1} NaH_2PO_4 and 1.25 mmol L^{-1} KH_2PO_4 in 1000 mL of distilled water; pH 7.4) for 1, 7, 14 and 28 days

(n = 3, in each time point). PBS was replaced every 7 days. After 1, 7, 14 and 28 days all the samples were dried in a vacuum desiccator. Surface of samples which exposed to blood or normal saline were characterized by X-ray diffractometer (XRD) and scanning electron microscope (SEM) with energy-dispersive X-ray spectroscopy (EDX) analyses. XRD analysis was performed first because this is a nondestructive technique. This was followed by SEM and EDX analyses.

X-ray diffraction analysis (XRD)

Phase analysis of materials was performed using a X-ray diffractometer (XRD; D8 Discover, Bruker, Karlsruhe, Germany) (Figure 6). The scan range was 10-65°2θ with a scan speed of 2°2θ per minute(113). Phase identification was accomplished using search match software using the ICDD database (International Centre for Diffraction Data, Newtown Square, PA).

Figure 6: X-ray diffractometer. (D8 Discover, Bruker, Karlsruhe, Germany)

Scanning electron microscope and Energy-dispersive X-ray spectroscopy (SEM and EDX analysis)

The samples were mounted on alumium stubs, pattinum coated and viewed with Scanning Electron Microscope (SEM; JSM-6610LV, JEOL, Tokyo, Japan) and Energy Dispersive X-Ray Spectroscopy (X-Max^{N} 50, Oxford instruments, Oxfordshire, United Kingdom) (Figure 7). Scanning electron micrographs of the material microstructural components were captured at 10,000x and EDX analysis was performed. EDX analysis was used to identify, quantify main composition of the samples (such as calcium, phosphorus, carbon, oxygen, silicon and other elements in trace amounts), which data were used to calculate the surface calcium-to-phosphorus atomic (Ca/P) ratios (stoichiometric hydroxyapatite Ca/P is 1.67) (45).

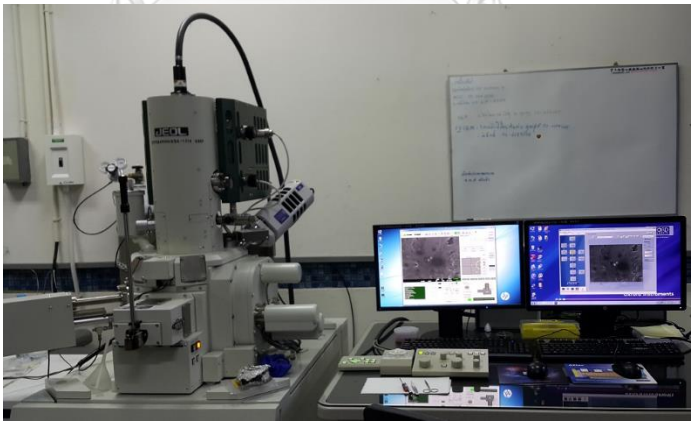

Figure 7: Scanning Electron Microscope (SEM; JSM-6610LV, JEOL, Tokyo, Japan) and Energy Dispersive X-Ray Spectroscopy (X-Max^{N} 50, Oxford instruments, Oxfordshire, United Kingdom)

Ion releasing analysis (calcium, silicon and phosphorus ion)

After setting, specimens were then immersed individually in plastic centrifuge containing 5 ml. of deionized water (n = 5 in each time point) (Figure 8). The evaluation periods were 1, 7, 14 and 28 days. Deionized water was renewed at the end of each time point.

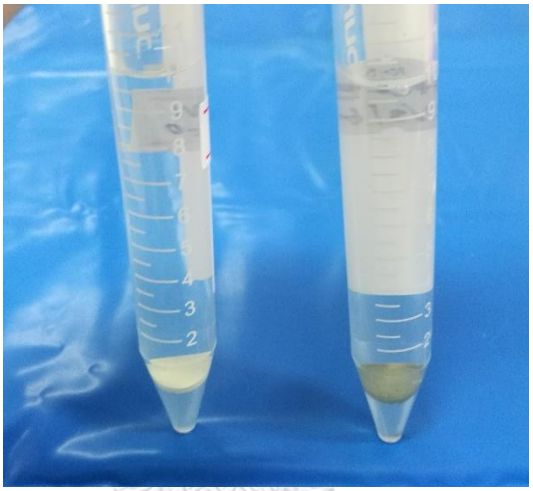

Figure 8: Each sample was immersed in deionized water.

The pH measurements were performed on the collected solutions with pH meter (model 710A, Thermo Scientific Orion, US). Calcium, Silicon and Phosphorus ion concentrations were measured through an Inductively Coupled Plasma Optical Emission Spectrometer (ICP-OES; model OPTIMA 7300DV, PerkinElmer, US).

Statistical analysis

pH values and ion concentration were expressed as mean and standard deviation. Two-way analysis of variance with the Student *t* test were used to determine

the statistical differences between the experimental groups using IBM SPSS software version 22 (IBM SPSS Inc, Chicago, IL, USA) at a significance level of 95%.

CHAPTER IV RESEARCH RESULTS

Chemical compositions analysis

MTA/non-blood; The XRD, SEM and EDX data of WMTA/non-blood was shown in Figure 9. At day 1, XRD analysis showed the phase of calcium carbonate ($Ca(CO_3)$, ICDD: 01-086-2334), calcium silicate oxide ($Ca_3(SiO_4)O$, ICDD: 01-073-0599) and bismuth oxide (alpha-Bi_2O_3, ICDD: 01-071-2274). SEM and EDX found small spherical precipitates over the surface and revealed elements of oxygen, carbon, calcium, silicon, phosphorus, sodium, bismuth and aluminium with Ca/P ratio of 5.62. At days 7, 14 and 28, large spherical precipitates had formed over the surface in SEM. EDX showed the increase of phosphorus and decrease of silicon, which Ca/P ratio decreased from 1.85 to 1.80. XRD analysis found hydroxyapatite ($Ca_{10}(PO_4)_6(OH)_2$, ICDD: 00-003-0747).

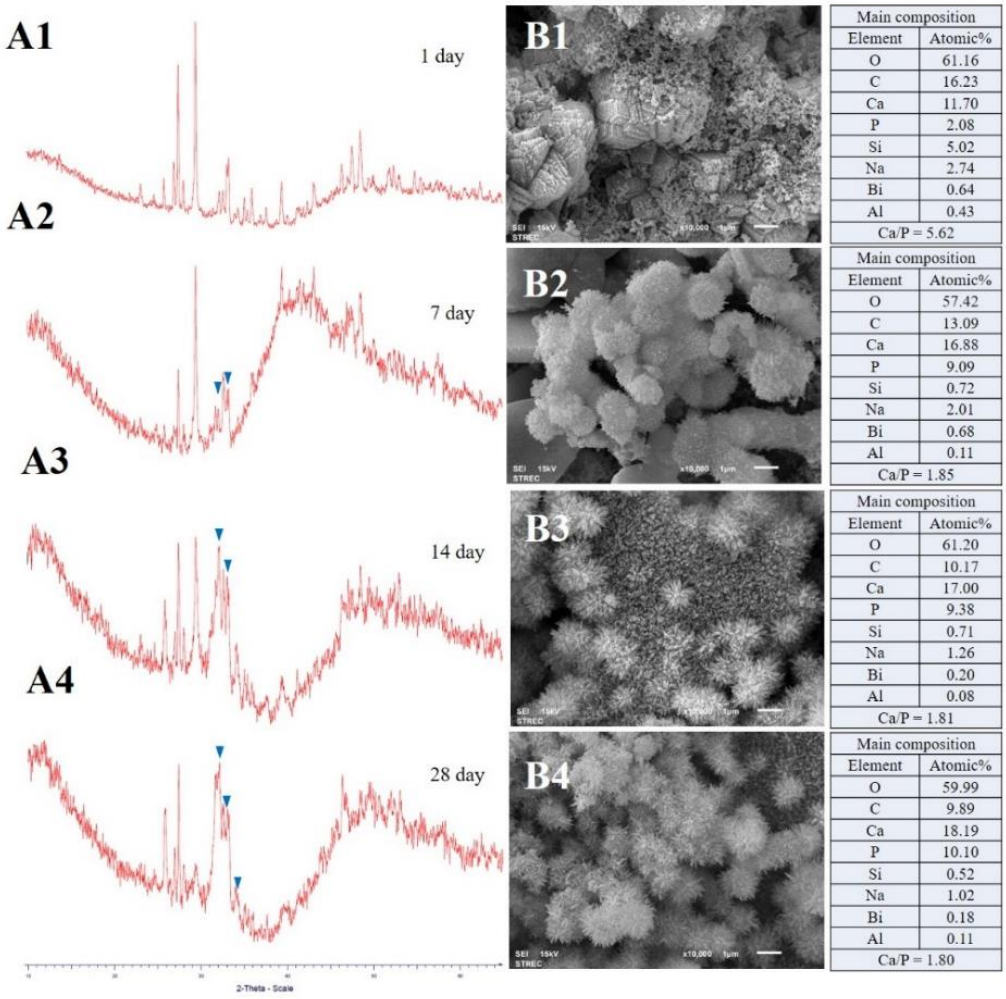

Main composition	
Element	Atomic%
O	61.16
C	16.23
Ca	11.70
P	2.08
Si	5.02
Na	2.74
Bi	0.64
Al	0.43
Ca/P = 5.62	

Main composition	
Element	Atomic%
O	57.42
C	13.09
Ca	16.88
P	9.09
Si	0.72
Na	2.01
Bi	0.68
Al	0.11
Ca/P = 1.85	

Main composition	
Element	Atomic%
O	61.20
C	10.17
Ca	17.00
P	9.38
Si	0.71
Na	1.26
Bi	0.20
Al	0.08
Ca/P = 1.81	

Main composition	
Element	Atomic%
O	59.99
C	9.89
Ca	18.19
P	10.10
Si	0.52
Na	1.02
Bi	0.18
Al	0.11
Ca/P = 1.80	

Figure 9: Chemical compositions of WMTA/non-blood after immersed in PBS for 1, 7, 14 and 28 days. (A1-A4) XRD analyasis of WMTA/non-blood. ▼= hydroxyapatite. (B1-B4) SEM and EDX analysis of WMTA/non-blood at x10,000 magnifications.

MTA/blood; The XRD, SEM and EDX data of WMTA/blood was shown in Figure 10. At day 1, XRD analysis displayed the phase of calcium carbonate, calcium silicate oxide and bismuth oxide. SEM found small spherical particles. EDX showed elements of oxygen, carbon, calcium, silicon, phosphorus, sodium, bismuth and aluminium with Ca/P ratio of 8.14. At days 7, XRD analysis showed the phases no noticeable difference. SEM found greater amount of small spherical particles. EDX displayed the increase of phosphorus and silicon with Ca/P ratio of 6.10. At days 14 and 28, large spherical precipitates had formed over the surface in SEM. EDX showed the increase of phosphorus and decrease of silicon, which Ca/P ratio decreased from 1.91 to 1.84. XRD analysis found hydroxyapatite.

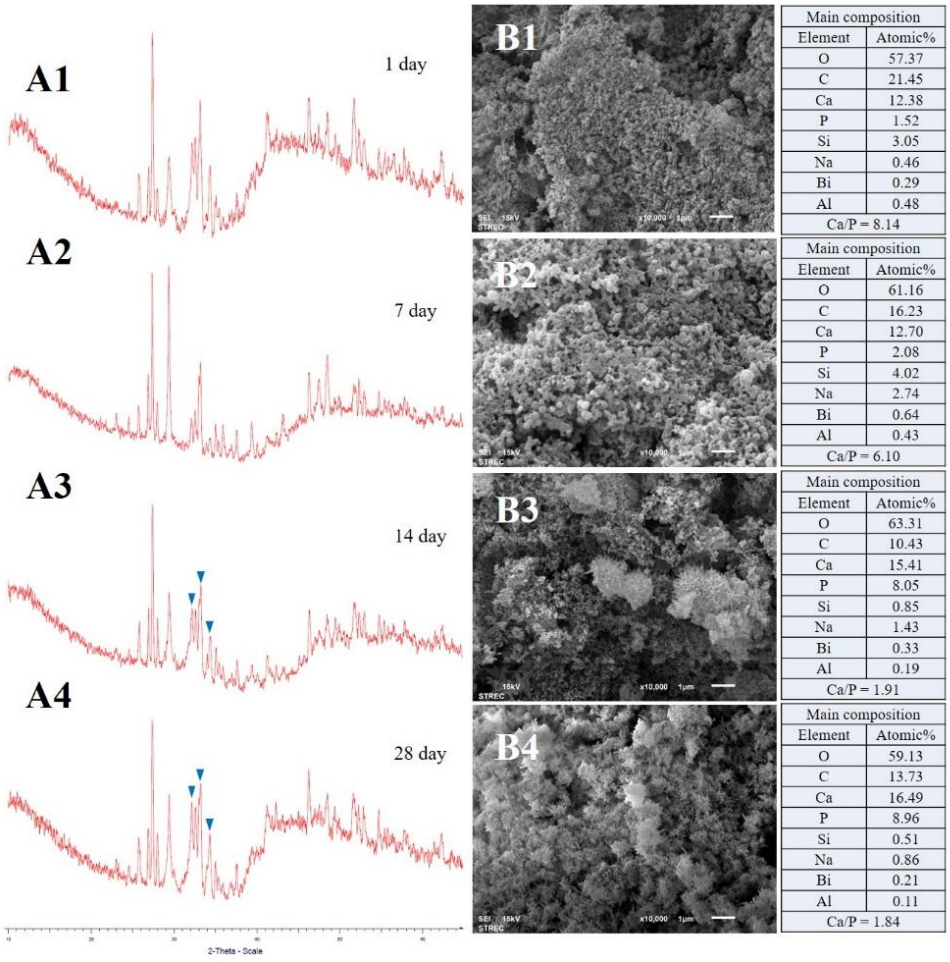

Main composition	
Element	Atomic%
O	57.37
C	21.45
Ca	12.38
P	1.52
Si	3.05
Na	0.46
Bi	0.29
Al	0.48
Ca/P = 8.14	

Main composition	
Element	Atomic%
O	61.16
C	16.23
Ca	12.70
P	2.08
Si	4.02
Na	2.74
Bi	0.64
Al	0.43
Ca/P = 6.10	

Main composition	
Element	Atomic%
O	63.31
C	10.43
Ca	15.41
P	8.05
Si	0.85
Na	1.43
Bi	0.33
Al	0.19
Ca/P = 1.91	

Main composition	
Element	Atomic%
O	59.13
C	13.73
Ca	16.49
P	8.96
Si	0.51
Na	0.86
Bi	0.21
Al	0.11
Ca/P = 1.84	

Figure 10: Chemical compositions of WMTA/blood after immersed in PBS for 1, 7, 14 and 28 days. (A1-A4) XRD analyasis of WMTA/blood. ▼ = hydroxyapatite. (B1-B4) SEM and EDX analysis of WMTA/blood at x10,000 magnifications.

Biodentine/non-blood; The XRD, SEM and EDX data of Biodentine/non-blood was shown in Figure 11. At day 1, XRD analysis displayed the phase of calcium carbonate, calcium silicate oxide and zirconium oxide (ZrO_2, ICDD: 01-074-1200). SEM found small granular particles and EDX revealed oxygen, carbon, calcium, silicon, phosphorus, sodium, zirconium and chloride with Ca/P ratio of 6.64. At days 7, XRD analysis showed the phases no noticeable difference. SEM found small spherical particles and EDX displayed increased phosphorus and silicon with Ca/P ratio of 4.99. At days 14 and 28, large spherical precipitates had formed over the surface in SEM and EDX displayed the increase of phosphorus and decrease of silicon, which Ca/P ratio decreased from 1.95 to 1.80. XRD analysis found hydroxyapatite.

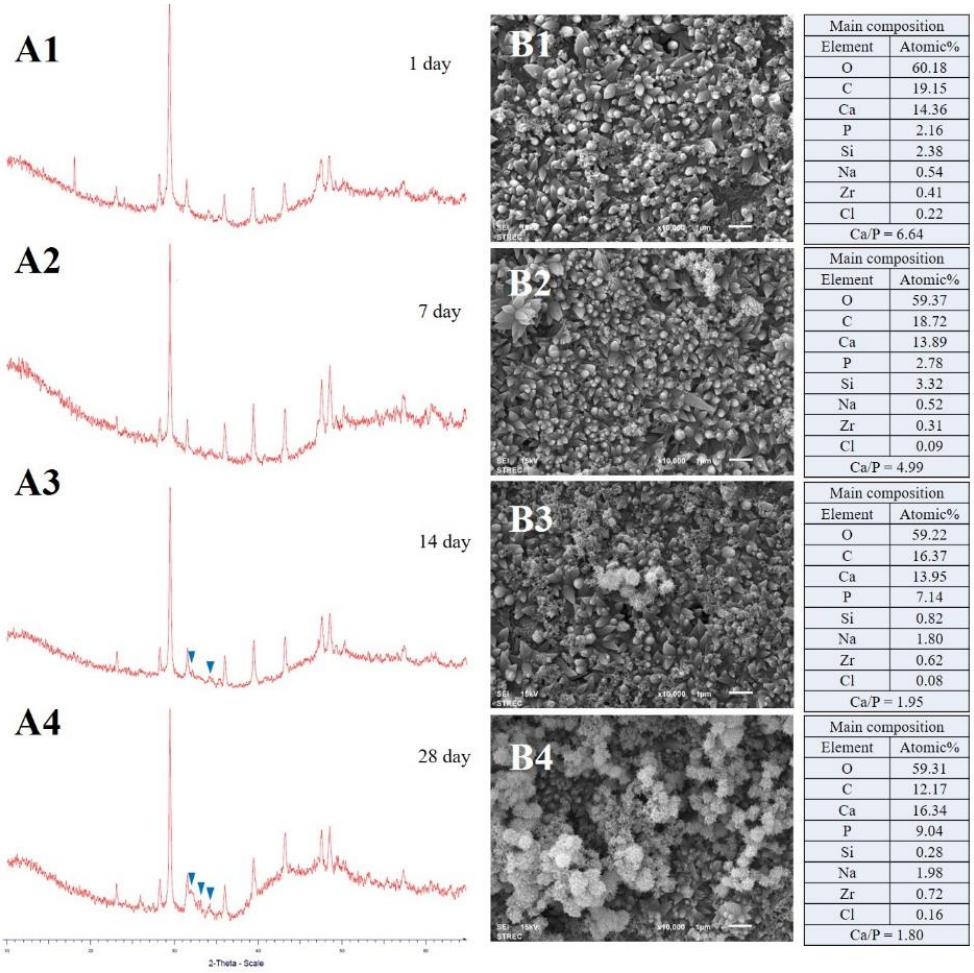

Main composition	
Element	Atomic%
O	60.18
C	19.15
Ca	14.36
P	2.16
Si	2.38
Na	0.54
Zr	0.41
Cl	0.22
Ca/P = 6.64	

Main composition	
Element	Atomic%
O	59.37
C	18.72
Ca	13.89
P	2.78
Si	3.32
Na	0.52
Zr	0.31
Cl	0.09
Ca/P = 4.99	

Main composition	
Element	Atomic%
O	59.22
C	16.37
Ca	13.95
P	7.14
Si	0.82
Na	1.80
Zr	0.62
Cl	0.08
Ca/P = 1.95	

Main composition	
Element	Atomic%
O	59.31
C	12.17
Ca	16.34
P	9.04
Si	0.28
Na	1.98
Zr	0.72
Cl	0.16
Ca/P = 1.80	

Figure 11: Chemical compositions of Biodentine/non-blood after immersed in PBS for 1, 7, 14 and 28 days. (A1-A4) XRD analyasis of Biodentine/non-blood. ▼ = hydroxyapatite. (B1-B4) SEM and EDX analysis of Biodentine/non-blood at x10,000 magnifications.

Biodentine/blood; The XRD, SEM and EDX data of Biodentine/blood was shown in Figure 12. At day 1, XRD analysis displayed the phase calcium carbonate, calcium silicate oxide and zirconium oxide. SEM found small spherical precipitates and EDX revealed elements of oxygen, carbon, calcium, silicon, phosphorus, sodium, zirconium and chloride with Ca/P ratio of 7.73. At days 7 and 14, XRD analysis showed the phases no noticeable difference. SEM found greater amount of small spherical precipitates and EDX displayed the increase of phosphorus and silicon with Ca/P ratio of 6.32 and 4.54. At days 28, large spherical precipitates had formed over the surface in SEM and EDX showed the increase of phosphorus and decrease of silicon, which Ca/P ratio decreased to 1.85. XRD analysis found hydroxyapatite.

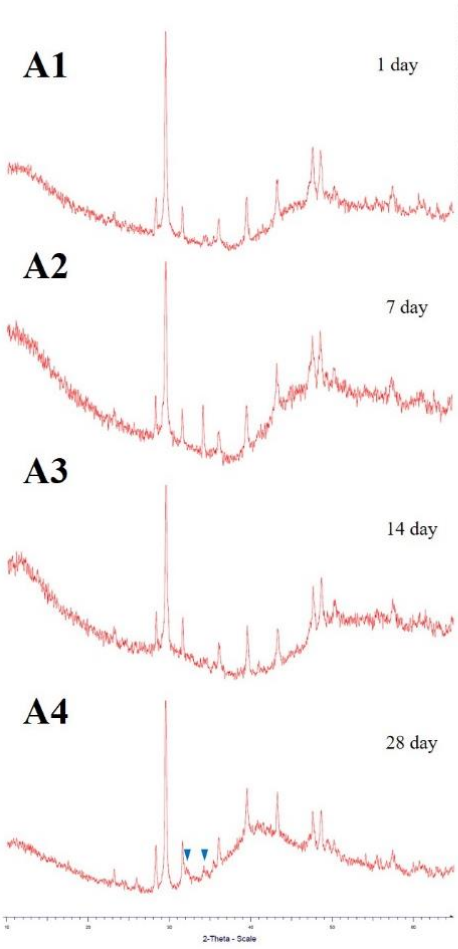

Main composition	
Element	Atomic%
O	59.56
C	23.31
Ca	12.84
P	1.66
Si	1.19
Na	0.85
Zr	0.38
Cl	0.21
Ca/P = 7.73	

Main composition	
Element	Atomic%
O	61.20
C	19.94
Ca	12.91
P	2.04
Si	2.66
Na	0.24
Zr	0.59
Cl	0.41
Ca/P = 6.32	

Main composition	
Element	Atomic%
O	59.61
C	18.25
Ca	14.01
P	3.08
Si	3.47
Na	0.93
Zr	0.40
Cl	0.18
Ca/P = 4.54	

Main composition	
Element	Atomic%
O	56.89
C	18.02
Ca	14.19
P	7.63
Si	0.65
Na	1.68
Zr	0.85
Cl	0.09
Ca/P = 1.85	

Figure 12: Chemical compositions of Biodentine/blood after immersed in PBS for 1, 7, 14 and 28 days. (A1-A4) XRD analyasis of Biodentine/blood. ▼ = hydroxyapatite. (B1-B4) SEM and EDX analysis of Biodentine/blood at x10,000 magnifications.

TRRM/non-blood; The XRD, SEM and EDX data of TRRM/non-blood was shown in Figure 13. At day 1, XRD analysis displayed the phase of calcium carbonate, calcium silicate oxide, zirconium oxide and tantalum oxide (Ta_2O_5, ICDD: 00-025-0922). SEM found small spherule particles and EDX showed elements of oxygen, carbon, calcium, silicon, phosphorus, sodium, zirconium and tantalum with Ca/P ratio of 11.31. At days 7, XRD analysis showed the phases no noticeable difference. SEM found greater amount of small spherical precipitates and EDX displayed the increase of phosphorus and silicon with Ca/P ratio of 5.04. At days 14 and 28, large spherical precipitates had formed over the surface in SEM and EDX showed the increase of phosphorus and decrease of silicon, which Ca/P ratio decreased from 1.89 to 1.81. XRD analysis found hydroxyapatite.

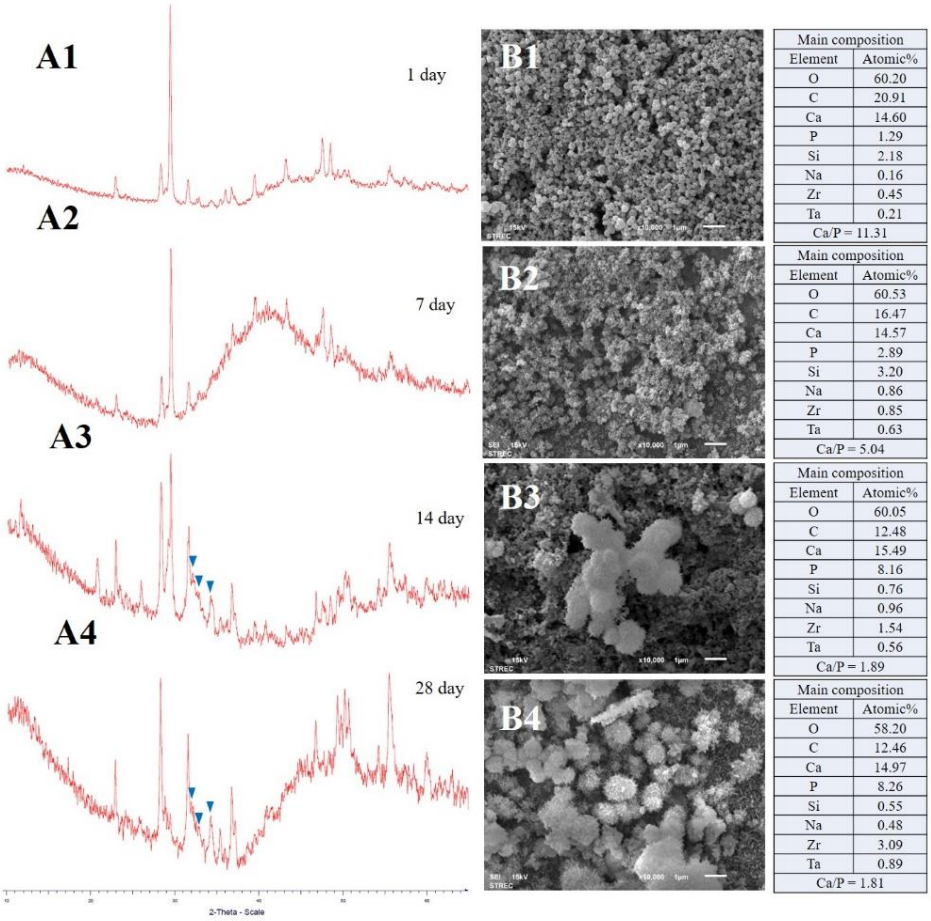

Main composition	
Element	Atomic%
O	60.20
C	20.91
Ca	14.60
P	1.29
Si	2.18
Na	0.16
Zr	0.45
Ta	0.21
Ca/P = 11.31	

Main composition	
Element	Atomic%
O	60.53
C	16.47
Ca	14.57
P	2.89
Si	3.20
Na	0.86
Zr	0.85
Ta	0.63
Ca/P = 5.04	

Main composition	
Element	Atomic%
O	60.05
C	12.48
Ca	15.49
P	8.16
Si	0.76
Na	0.96
Zr	1.54
Ta	0.56
Ca/P = 1.89	

Main composition	
Element	Atomic%
O	58.20
C	12.46
Ca	14.97
P	8.26
Si	0.55
Na	0.48
Zr	3.09
Ta	0.89
Ca/P = 1.81	

Figure 13: Chemical compositions of TRRM/non-blood after immersed in PBS for 1, 7, 14 and 28 days. (A1-A4) XRD analyasis of TRRM/non-blood. ▼= hydroxyapatite. (B1-B4) SEM and EDX analysis of TRRM/non-blood at x10,000 magnifications.

TRRM/blood; The XRD, SEM and EDX data of TRRM/blood was shown in Figure 14. At day 1, XRD analysis displayed the phase calcium carbonate, calcium silicate oxide, zirconium oxide and tantalum oxide. SEM found greater amount of small spherical precipitates and EDX revealed oxygen, carbon, calcium, silicon, phosphorus, sodium, zirconium and chloride with Ca/P ratio of 10.10. At days 7 and 14, XRD analysis showed the phases no noticeable difference. SEM found small spherical precipitates and EDX displayed the increase of phosphorus and silicon with Ca/P ratio of 5.13 and 4.39. At days 28, spherical precipitates had formed over the surface in SEM and EDX showed the increase of phosphorus and decrease of silicon, which Ca/P ratio decreased to 1.93. XRD analysis found hydroxyapatite.

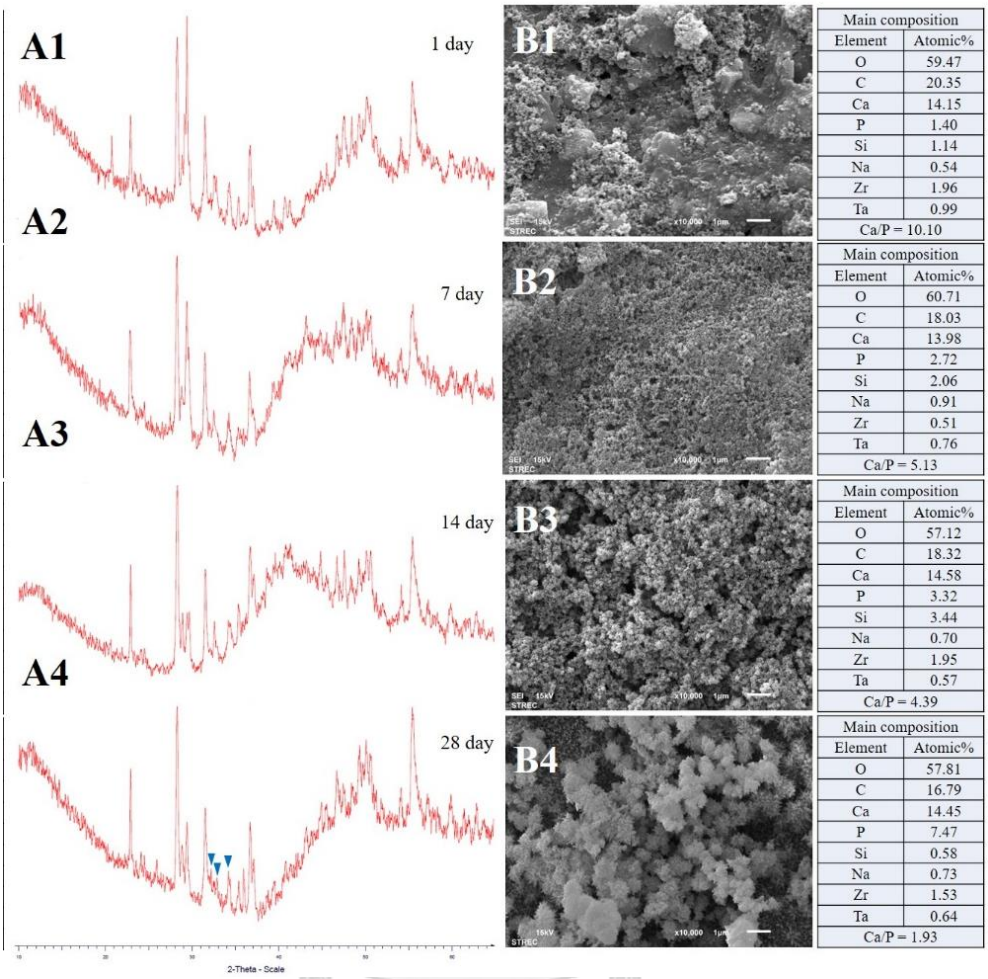

Main composition	
Element	Atomic%
O	59.47
C	20.35
Ca	14.15
P	1.40
Si	1.14
Na	0.54
Zr	1.96
Ta	0.99
Ca/P = 10.10	

Main composition	
Element	Atomic%
O	60.71
C	18.03
Ca	13.98
P	2.72
Si	2.06
Na	0.91
Zr	0.51
Ta	0.76
Ca/P = 5.13	

Main composition	
Element	Atomic%
O	57.12
C	18.32
Ca	14.58
P	3.32
Si	3.44
Na	0.70
Zr	1.95
Ta	0.57
Ca/P = 4.39	

Main composition	
Element	Atomic%
O	57.81
C	16.79
Ca	14.45
P	7.47
Si	0.58
Na	0.73
Zr	1.53
Ta	0.64
Ca/P = 1.93	

Figure 14: Chemical compositions of TRRM/blood after immersed in PBS for 1, 7, 14 and 28 days. (A1-A4) XRD analyasis of TRRM/blood. ▼ = hydroxyapatite. (B1-B4) SEM and EDX analysis of TRRM/blood at x10,000 magnifications.

Ion releasing analysis

pH. pH of test materials immersed in deionized water for 1, 7, 14 and 28 days was displayed in Table 4. All test materials exhibited an alkaline pH in every evaluation time points (11.03-12.14). For all groups, pH value increased to a maximum level at days 7 and then gradually decreased at days 14 to 28. There were no significant differences between conditions of the same material. However, Biodentine and TRRM displayed significantly higher pH than WMTA ($P < .05$) at all time points in both conditions.

Table 4: pH of test materials when immersed in deionized water.

Period (day)	WMTA /non-blood	WMTA /blood	Biodentine /non-blood	Biodenine /blood	TRRM /non-blood	TRRM /blood
1	11.24 ± 0.2[a]	11.36 ± 0.11[a]	11.47 ± 0.06[b]	11.43 ± 0.04[b]	11.46 ± 0.07[b]	11.51 ± 0.04[b]
7	11.49 ± 0.22[a]	11.67 ± 0.12[a]	12.05 ± 0.08[b]	12.07 ± 0.11[b]	12.12 ± 0.03[b]	12.14 ± 0.03[b]
14	11.27 ± 0.25[a]	11.32 ± 0.21[a]	11.73 ± 0.2[b]	11.83 ± 0.01[b]	11.69 ± 0.14[b]	11.7 ± 0.15[b]
28	11.03 ± 0.34[a]	11.3 ± 0.21[a]	11.63 ± 0.1[b]	11.59 ± 0.07[b]	11.55 ± 0.1[b]	11.41 ± 0.15[b]

Mean ± SD, $n = 5$.

Mean values followed by different superscripted letters were significantly different ($P < .05$)

Calcium Ion Release. Calcium ion release of test materials immersed in deionized water for 1, 7, 14 and 28 days was shown in Table 5. In all groups, the calcium ion release increased to a maximum level at days 7 and then gradually decreased at days 14 to 28. There were no significant differences between conditions of the same material.

However, Biodentine showed significantly higher calcium ion release than WMTA at all time points ($P < .05$) and showed significantly higher calcium ion than TRRM at days 1 and 28 ($P < .05$).

Table 5: Calcium ion release (mg/L) of test materials when immersed in deionized water.

Period (day)	MTA /non-blood	MTA /blood	Biodentine /non-blood	Biodentine /blood	TRRM /non-blood	TRRM /blood
1	32.24 ± 18.01^{a}	52.76 ± 39.27^{a}	184.92 ± 41.22^{b}	190.08 ± 23.53^{b}	62.32 ± 32.38^{a}	74.25 ± 22.39^{a}
7	66.55 ± 56.72^{a}	84.71 ± 12.93^{a}	215.3 ± 31.33^{b}	197.58 ± 57.24^{b}	195.36 ± 13.15^{b}	193.1 ± 30.91^{b}
14	60.69 ± 39.13^{a}	72.39 ± 57.72^{a}	159.73 ± 54.09^{b}	160.73 ± 52.76^{b}	124.97 ± 33.87^{ab}	121.74 ± 32.59^{ab}
28	38.82 ± 22.69^{a}	39.96 ± 8.12^{a}	114.83 ± 23.29^{b}	113.3 ± 32.15^{b}	83.22 ± 18.1^{c}	65.82 ± 18.55^{c}

Mean ± SD, $n = 5$.

Mean values followed by different superscripted letters were significantly different ($P < .05$)

Silicon Ion Release. Silicon ion release of test materials immersed in deionized water for 1, 7, 14 and 28 days was shown in Table 6. In all groups, the silicon ion release increased to a maximum level at days 7 and then gradually decreased. There were significant differences both conditions and materials in each time point. In non-blood-contaminated groups, all materials displayed significantly higher silicon ion release than blood-contaminated groups ($P < .05$). The WMTA/non-blood group exhibited significantly higher silicon ion release than other groups at all time points ($P < .05$).

Table 6: Silicon ion release (mg/L) of test materials when immersed in deionized water.

Period (day)	MTA /non-blood	MTA /blood	Biodentine /non-blood	Biodentine /blood	TRRM /non-blood	TRRM /blood
1	1.21 ± 0.12^{a}	0.87 ± 0.13^{b}	0.8 ± 0.1^{b}	0.41 ± 0.14^{c}	0.78 ± 0.07^{b}	0.48 ± 0.09^{c}
7	1.64 ± 0.18^{a}	1.11 ± 0.2^{b}	0.94 ± 0.13^{b}	0.64 ± 0.13^{c}	0.96 ± 0.12^{b}	0.57 ± 0.14^{c}
14	1.4 ± 0.2^{a}	0.76 ± 0.18^{b}	0.83 ± 0.13^{b}	0.44 ± 0.08^{c}	0.76 ± 0.11^{b}	0.49 ± 0.04^{c}
28	1.49 ± 0.25^{a}	0.85 ± 0.15^{b}	0.79 ± 0.14^{b}	0.4 ± 0.05^{c}	0.7 ± 0.12^{b}	0.41 ± 0.08^{c}

Mean ± SD, n = 5.

Mean values followed by different superscripted letters were significantly different ($P < .05$)

Phosphorus Ion Release. We could not detect phosphorus ion release in all samples.

CHAPTER V DISCUSSION

The present study tested three calcium silicate-based materials that were introduced on the market to compare the effect of blood contamination on chemical compositions and ion release. The null hypothesis was disproved because there was difference between blood-contaminated groups and no blood-contaminated groups in chemical compositions and silicon ion release.

The study about the composition of the structures of materials requires various methods including microstructures, elemental analysis and phase analysis. SEM is suited for the study of microstructures. EDX allows qualitative analysis of the elements, but these technique does not identify the phases of materials. In present study, XRD identifies the main phases related to the materials. This study showed that all specimen surfaces exhibited precipitation of spherical clusters after being immersed in PBS. EDX and XRD confirmed that the observed spherical precipitates were apatite precipitates. In this study, when we detected apatite from XRD, while the increase of calcium and phosphorus were simultaneously shown in EDX with Ca/P ratio similar to stoichiometric hydroxyapatite (114). High calcium and phosphorus are connected with the formation of apatite deposits because apatite mainly consists of calcium phosphate phase (114).

When exposed to phosphate-containing solution, calcium silicate-based materials can form apatite crystals (5, 8). Our result showed that all test materials

presented the ability to form apatite after being immersed in PBS. Moreover, the current study showed that WMTA displayed earlier precipitation than Biodentine and TRRM in both conditions. After immersed in PBS for 7 days, apatite was only detected in the WMTA/non-blood group. In previous studies, apatite precipitates had been observed on MTA, Biodentine and EndoSequence Root Repair Material (ERRM) surfaces after immersed in phosphate-buffer solution (11, 27, 81). The importance of hydroxyapatite in supporting osteoblastic differentiation which leads to bone bonding is well known (92). The presence of an extensive apatite layer on biomaterials promotes the adsorption of proteins and the formation of a protein layer that favors osteoblast adhesion (94, 115). Moreover, their deposition over time improved sealing at the interface between dentin and materials (5). Therefore, the delay of apatite formation that may affect osteoblast behaviour and sealing ability between dentin and materials. Further studies are required to examine hard tissue formation of calcium silicated-based materials in blood-contaminated condition.

The products of the chemical reactions between the materials and solutions formed an apatite layer on the calcium silicate-based materials. During hydration reaction, silanol groups (Si-OH) on calcium silicate hydrate are deprotonated at alkaline environment. Negative charges surface (SiO^-) interacted with calcium ions, resulting in an increase of cations on the set cement surface that act as nucleation sites for apatite formation from the amorphous calcium phosphate (96). The current study showed that precipitation of apatite was found later in blood-contaminated specimens than non-blood-contaminated specimens. Furthermore, prior to detecting apatite formation, blood-contaminated groups displayed a lower silicon atomic percentage compared with non-blood-contaminated groups and slowly increased over time until apatite was found. Thus, blood might impede silicon on material's surface during the hydration reaction leading to delayed apatite formation.

The presence of silicon was found to be crucial for a material to exhibit bioactivity (116). Dissolving the material in an alkaline environment releases silicon ion that form the silica gel surface layer in calcium silicate hydrate gel and creates silanol

groups to act as sites for the nucleation of apatite from the amorphous calcium phosphate deposited over the silica gel layer (116). Our results indicated that for each material, the non-blood-contaminated groups' silicon ion release was significantly higher compared with the blood-contaminated groups'. These results suggest that blood may reduce silicon ion release, inhibiting the development of the silica gel layer on the material's surface. The role of silicon ions in hard tissue formation was suggested in early bone calcification and inhibition of osteoclastogenesis (117, 118). Moreover silicon is reported to induce remineralization of demineralized dentine *in vitro* (119). Our study showed that the release of silicon ions from WMTA was greater compared with Biodentine and TRRM in both conditions. Increased silicon ion release facilitates osteoblast differentiation and inhibits osteoclastogenesis, thus promoting the healing of periapical tissues (118, 120). However, whether the reduced silicon ion release in blood-contaminated calcium silicate-based materials has an impact on hard tissue formation requires further study.

The setting reaction of calcium silicate-based materials involves the hydration reaction of calcium silicates which results in the production of calcium hydroxide, that creates a highly alkaline environment and the major source of calcium ion released from these materials (108). Although these reactions occur almost immediately after cement hydration, continuous release of calcium ion and silicon ion after initial setting which result in the formation of apatite. Our study demonstrated that all test materials released calcium and silicon ions and maintained an alkaline pH that reached its maximum value at day 7 and decreased over time. In current study showed that pH value and calcium ion release, there were no significant differences between conditions, but there were statistically significant difference between materials. WMTA's calcium ion release pattern is comparable to that in a previous study, Camilleri (59) showed WMTA produced calcium ions from calcium hydroxide, a by-product of hydration, and also by decomposition of calcium silicate hydrate. The release of calcium ions reduced with time (maximum at 1 week and gradually decreased until 5 week). Our results demonstrated that Biodentine and TRRM had a higher pH and calcium ion release

compared with WMTA at all experimental time points. This finding is similar to a previous report by Han and Okiji (81). They compared the amount of calcium ion release from WMTA, Biodentine and EndoSequence BC sealer, and found that Biodentine showed calcium ion release when immersed in distilled water more than WMTA (0-5, 5-24, 24-48, 144-168 hours). In this regard, the higher calcium ion release from Biodentine may be attributable to its calcium chloride added as an accelerator (121). It has been demonstrated, by both *in vitro* and *in vivo* studies, that the mechanism of pulp wound healing by the deposition of mineralized apatite depends on pH and the ability of calcium ion release (122, 123)

The amount of phosphorus ion release could not be detected when all materials immersed in deionized water. This study confirmed that all test materials did not have the ability to release phosphorus ion. The peak of phosphorus from EDS that detected on surface of materials were derived from PBS.

According to the pilot study, all test materials were placed in a polytetrafluoroethylene mold. After 24 hours in an incubator, we found that TRRM did not

set. This could be due to TRRM requires continuous exposure to moisture during setting. Therefore, in this study the plaster of Paris mold were stored at 37 ºC and >95% relative humidity for 24 hours before placing the materials as reported in previous studies (124, 125). Plaster of paris is calcium sulphate hemihydrate which may affect chemical composition and ion releasing of test materials. Therefore, to control this variable, the plaster of Paris mold were used in all test materials.

In the majority of endodontic applications, the material comes into contact with blood during placement. Many previous studies investigated MTA's properties when it was mixed with blood (84, 85, 126). However, mixing MTA with blood represents a situation that may be far from the clinical reality in which the material comes into contact with fluids after placing into the cavity. This study exposed the materials to human whole fresh blood immediately after mixing by placing them into the mold filled to most closely simulate the clinical conditions.

In the present study, whole fresh blood was collected from healthy volunteer in heparin tube. The advantage of using fresh, human blood is that it more closely

replicates the human clinical situation. Whole fresh human blood has been widely used in other studies (84, 85, 126). However, experiments involving whole, fresh human blood present difficulties such as ethical considerations, biohazard issues and obtaining sufficient volumes of blood over a prolonged period of time without the addition of anticoagulant agents.

Based on these findings, we hypothesize that blood contamination of calcium silicate-based materials interrupts ion exchange during hydration and reduces the formation of the silanol groups that act as sites for nucleation of apatite. Blood exposure reduces a material's silicon ion release. Therefore, blood may inhibit the development of a silica gel layer on a material's surface. WMTA demonstrated earlier apatite formation and greater silicon ion release compared with Biodentine and TRRM when exposed to blood. In conclusion, blood contamination delayed apatite formation and decreased silicon ion release of calcium silicate-based materials, but not their pH or calcium ion release. Thus, hemorrhage control is recommended before placing the materials in clinical situations.

Limitations

Although XRD analysis can be performed for identification of crystalline phase, the substantial peak overlap caused by the large number of phases present in the material may occur.

This is a laboratory study, it may not represent clinical situation and outcomes. Further *in vivo* or clinical studies will provide better understanding of outcome of these novel repair materials.

APPENDIX A

pH

Table 7: Descriptive Statistics: pH of day 1

materials	contaminate	Mean	Std. Deviation	N
WMTA	Non-blood	11.2480	.20204	5
	blood	11.3680	.11167	5
	Total	11.3080	.16639	10
Biodentine	Non-blood	11.4740	.06348	5
	blood	11.4320	.04868	5
	Total	11.4530	.05774	10
TRRM	Non-blood	11.4620	.07259	5
	blood	11.5160	.04722	5
	Total	11.4890	.06437	10
Total	Non-blood	11.3947	.16084	15
	blood	11.4387	.09387	15
	Total	11.4167	.13132	30

Table 8: Tests of Between-Subjects Effects: pH of day 1

Source	Type III Sum of Squares	df	Mean Square	F	Sig.
Corrected Model	.231[a]	5	.046	4.131	.008
Intercept	3910.208	1	3910.208	349177.705	.000
materials	.184	2	.092	8.198	.002
contaminate	.015	1	.015	1.297	.266
materials * contaminate	.033	2	.017	1.481	.247
Error	.269	24	.011		
Total	3910.708	30			
Corrected Total	.500	29			

a. R Squared = .463 (Adjusted R Squared = .351)

Table 9: Pairwise Comparisons: pH of day 1

(I) materials	(J) materials	Mean Difference (I-J)	Std. Error	Sig.[b]	95% Confidence Interval for Difference[b]	
					Lower Bound	Upper Bound
WMTA	Biodentine	-.145*	.047	.016	-.267	-.023
	TRRM	-.181*	.047	.002	-.303	-.059
Biodentine	WMTA	.145*	.047	.016	.023	.267
	TRRM	-.036	.047	1.000	-.158	.086
TRRM	WMTA	.181*	.047	.002	.059	.303
	Biodentine	.036	.047	1.000	-.086	.158

Based on estimated marginal means

*. The mean difference is significant at the .05 level.

b. Adjustment for multiple comparisons: Bonferroni.

Table 10: Pairwise Comparisons: pH of day 1

(I) contaminate	(J) contaminate	Mean Difference (I-J)	Std. Error	Sig.[a]	95% Confidence Interval for Difference[a]	
					Lower Bound	Upper Bound
Non-blood	blood	-.044	.039	.266	-.124	.036
blood	Non-blood	.044	.039	.266	-.036	.124

Based on estimated marginal means

a. Adjustment for multiple comparisons: Bonferroni.

Table 11: Descriptive Statistics: pH of day 7

materials	contaminate	Mean	Std. Deviation	N
WMTA	Non-blood	11.4960	.22367	5
	blood	11.6700	.12865	5
	Total	11.5830	.19494	10
Biodentine	Non-blood	12.0540	.08849	5
	blood	12.0760	.11524	5
	Total	12.0650	.09755	10
TRRM	Non-blood	12.1220	.03421	5
	blood	12.1440	.03286	5
	Total	12.1330	.03368	10
Total	Non-blood	11.8907	.31802	15
	blood	11.9633	.23612	15
	Total	11.9270	.27768	30

Table 12: Tests of Between-Subjects Effects: pH of day 7

Source	Type III Sum of Squares	df	Mean Square	F	Sig.
Corrected Model	1.876[a]	5	.375	25.034	.000
Intercept	4267.600	1	4267.600	284696.456	.000
materials	1.798	2	.899	59.979	.000
contaminate	.040	1	.040	2.642	.117
materials * contaminate	.039	2	.019	1.284	.295
Error	.360	24	.015		
Total	4269.836	30			
Corrected Total	2.236	29			

a. R Squared = .839 (Adjusted R Squared = .806)

Table 13: Pairwise Comparisons: pH of day 7

(I) materials	(J) materials	Mean Difference (I-J)	Std. Error	Sig.[b]	95% Confidence Interval for Difference[b]	
					Lower Bound	Upper Bound
WMTA	Biodentine	-.482*	.055	.000	-.623	-.341
	TRRM	-.550*	.055	.000	-.691	-.409
Biodentine	WMTA	.482*	.055	.000	.341	.623
	TRRM	-.068	.055	.679	-.209	.073
TRRM	WMTA	.550*	.055	.000	.409	.691
	Biodentine	.068	.055	.679	-.073	.209

Based on estimated marginal means

*. The mean difference is significant at the .05 level.

b. Adjustment for multiple comparisons: Bonferroni.

Table 14: Pairwise Comparisons: pH of day 7

(I) contaminate	(J) contaminate	Mean Difference (I-J)	Std. Error	Sig.[a]	95% Confidence Interval for Difference[a]	
					Lower Bound	Upper Bound
Non-blood	blood	-.073	.045	.117	-.165	.020
blood	Non-blood	.073	.045	.117	-.020	.165

Based on estimated marginal means

a. Adjustment for multiple comparisons: Bonferroni.

Table 15: Descriptive Statistics: pH of day 14

materials	contaminate	Mean	Std. Deviation	N
WMTA	Non-blood	11.2760	.25026	5
	blood	11.3200	.20976	5
	Total	11.2980	.21893	10
Biodentine	Non-blood	11.7300	.20457	5
	blood	11.8340	.01673	5
	Total	11.7820	.14741	10
TRRM	Non-blood	11.6980	.14220	5
	blood	11.7060	.15323	5
	Total	11.7020	.13943	10
Total	Non-blood	11.5680	.28546	15
	blood	11.6200	.26552	15
	Total	11.5940	.27216	30

Table 16: Tests of Between-Subjects Effects: pH of day 14

Source	Type III Sum of Squares	df	Mean Square	F	Sig.
Corrected Model	1.378[a]	5	.276	8.594	.000
Intercept	4032.625	1	4032.625	125718.334	.000
materials	1.346	2	.673	20.985	.000
contaminate	.020	1	.020	.632	.434
materials * contaminate	.012	2	.006	.183	.834
Error	.770	24	.032		
Total	4034.773	30			
Corrected Total	2.148	29			

a. R Squared = .642 (Adjusted R Squared = .567)

Table 17: Pairwise Comparisons: pH of day 14

(I) materials	(J) materials	Mean Difference (I-J)	Std. Error	Sig.[b]	95% Confidence Interval for Difference[b]	
					Lower Bound	Upper Bound
WMTA	Biodentine	-.484*	.080	.000	-.690	-.278
	TRRM	-.404*	.080	.000	-.610	-.198
Biodentine	WMTA	.484*	.080	.000	.278	.690
	TRRM	.080	.080	.984	-.126	.286
TRRM	WMTA	.404*	.080	.000	.198	.610
	Biodentine	-.080	.080	.984	-.286	.126

Based on estimated marginal means

*. The mean difference is significant at the .05 level.

b. Adjustment for multiple comparisons: Bonferroni.

Table 18: Pairwise Comparisons: pH of day 14

(I) contaminate	(J) contaminate	Mean Difference (I-J)	Std. Error	Sig.[a]	95% Confidence Interval for Difference[a]	
					Lower Bound	Upper Bound
Non-blood	blood	-.052	.065	.434	-.187	.083
blood	Non-blood	.052	.065	.434	-.083	.187

Based on estimated marginal means

a. Adjustment for multiple comparisons: Bonferroni.

Table 19: Descriptive Statistics: pH of day 28

materials	contaminate	Mean	Std. Deviation	N
WMTA	Non-blood	11.0380	.34824	5
	blood	11.3000	.21178	5
	Total	11.1690	.30479	10
Biodentine	Non-blood	11.6320	.10426	5
	blood	11.5940	.07668	5
	Total	11.6130	.08858	10
TRRM	Non-blood	11.5500	.10607	5
	blood	11.4180	.15320	5
	Total	11.4840	.14238	10
Total	Non-blood	11.4067	.33909	15
	blood	11.4373	.19193	15
	Total	11.4220	.27117	30

Table 20: Tests of Between-Subjects Effects: pH of day 28

Source	Type III Sum of Squares	df	Mean Square	F	Sig.
Corrected Model	1.262[a]	5	.252	6.961	.000
Intercept	3913.863	1	3913.863	107923.963	.000
materials	1.043	2	.522	14.385	.000
contaminate	.007	1	.007	.194	.663
materials * contaminate	.212	2	.106	2.919	.073
Error	.870	24	.036		
Total	3915.995	30			
Corrected Total	2.132	29			

a. R Squared = .592 (Adjusted R Squared = .507)

Table 21: Pairwise Comparisons; pH of day 28

(I) materials	(J) materials	Mean Difference (I-J)	Std. Error	Sig.[b]	95% Confidence Interval for Difference[b]	
					Lower Bound	Upper Bound
WMTA	Biodentine	-.444*	.085	.000	-.663	-.225
	TRRM	-.315*	.085	.003	-.534	-.096
Biodentine	WMTA	.444*	.085	.000	.225	.663
	TRRM	.129	.085	.429	-.090	.348
TRRM	WMTA	.315*	.085	.003	.096	.534
	Biodentine	-.129	.085	.429	-.348	.090

Based on estimated marginal means

*. The mean difference is significant at the .05 level.

b. Adjustment for multiple comparisons: Bonferroni.

Table 22: Pairwise Comparisons: pH of day 28

(I) contaminate	(J) contaminate	Mean Difference (I-J)	Std. Error	Sig.[a]	95% Confidence Interval for Difference[a]	
					Lower Bound	Upper Bound
Non-blood	blood	-.031	.070	.663	-.174	.113
blood	Non-blood	.031	.070	.663	-.113	.174

Based on estimated marginal means

a. Adjustment for multiple comparisons: Bonferroni.

APPENDIX B

Calcium ion release

Table 23: Descriptive Statistics: calcium ion release of day 1

materials	contaminate	Mean	Std. Deviation	N
WMTA	Non-blood	32.24540	18.018468	5
	blood	52.76200	39.279291	5
	Total	42.50370	30.772352	10
Biodentine	Non-blood	184.92000	41.221863	5
	blood	190.08000	23.539584	5
	Total	187.50000	31.762976	10
TRRM	Non-blood	62.32600	32.388700	5
	blood	74.25800	22.392284	5
	Total	68.29200	26.993210	10
Total	Non-blood	93.16380	74.497291	15
	blood	105.70000	68.111586	15
	Total	99.43190	70.423633	30

Table 24: Tests of Between-Subjects Effects: calcium ion release of day 1

Source	Type III Sum of Squares	df	Mean Square	F	Sig.
Corrected Model	121139.858[a]	5	24227.972	25.632	.000
Intercept	296601.082	1	296601.082	313.790	.000
materials	119665.036	2	59832.518	63.300	.000
contaminate	1178.672	1	1178.672	1.247	.275
materials * contaminate	296.150	2	148.075	.157	.856
Error	22685.297	24	945.221		
Total	440426.237	30			
Corrected Total	143825.155	29			

a. R Squared = .842 (Adjusted R Squared = .809)

Table 25: Pairwise Comparisons: calcium ion release of day 1

(I) materials	(J) materials	Mean Difference (I-J)	Std. Error	Sig.[b]	95% Confidence Interval for Difference[b]	
					Lower Bound	Upper Bound
WMTA	Biodentine	-144.996*	13.749	.000	-180.382	-109.610
	TRRM	-25.788	13.749	.219	-61.174	9.598
Biodentine	WMTA	144.996*	13.749	.000	109.610	180.382
	TRRM	119.208*	13.749	.000	83.822	154.594
TRRM	WMTA	25.788	13.749	.219	-9.598	61.174
	Biodentine	-119.208*	13.749	.000	-154.594	-83.822

Based on estimated marginal means

*. The mean difference is significant at the .05 level.

b. Adjustment for multiple comparisons: Bonferroni.

Table 26: Pairwise Comparisons: calcium ion release of day 1

(I) contaminate	(J) contaminate	Mean Difference (I-J)	Std. Error	Sig.[a]	95% Confidence Interval for Difference[a]	
					Lower Bound	Upper Bound
Non-blood	blood	-12.536	11.226	.275	-35.706	10.634
blood	Non-blood	12.536	11.226	.275	-10.634	35.706

Based on estimated marginal means

a. Adjustment for multiple comparisons: Bonferroni.

Table 27: Descriptive Statistics: calcium ion release of day 7

materials	contaminate	Mean	Std. Deviation	N
WMTA	Non-blood	66.55400	56.722870	5
	blood	84.71800	12.936979	5
	Total	75.63600	39.950281	10
Biodentine	Non-blood	215.30000	31.332332	5
	blood	197.58000	57.244100	5
	Total	206.44000	44.496447	10
TRRM	Non-blood	195.36000	13.151540	5
	blood	193.10000	30.914317	5
	Total	194.23000	22.428655	10
Total	Non-blood	159.07133	76.847987	15
	blood	158.46600	64.609111	15
	Total	158.76867	69.758711	30

Table 28: Tests of Between-Subjects Effects: calcium ion release of day 7

Source	Type III Sum of Squares	df	Mean Square	F	Sig.
Corrected Model	106033.617[a]	5	21206.723	14.505	.000
Intercept	756224.685	1	756224.685	517.247	.000
materials	104411.025	2	52205.512	35.708	.000
contaminate	2.748	1	2.748	.002	.966
materials * contaminate	1619.844	2	809.922	.554	.582
Error	35088.437	24	1462.018		
Total	897346.740	30			
Corrected Total	141122.054	29			

a. R Squared = .751 (Adjusted R Squared = .700)

Table 29: Pairwise Comparisons: calcium ion release of day 7

(I) materials	(J) materials	Mean Difference (I-J)	Std. Error	Sig.[b]	95% Confidence Interval for Difference[b]	
					Lower Bound	Upper Bound
WMTA	Biodentine	-130.804*	17.100	.000	-174.813	-86.795
	TRRM	-118.594*	17.100	.000	-162.603	-74.585
Biodentine	WMTA	130.804*	17.100	.000	86.795	174.813
	TRRM	12.210	17.100	1.000	-31.799	56.219
TRRM	WMTA	118.594*	17.100	.000	74.585	162.603
	Biodentine	-12.210	17.100	1.000	-56.219	31.799

Based on estimated marginal means

*. The mean difference is significant at the .05 level.

b. Adjustment for multiple comparisons: Bonferroni.

Table 30: Pairwise Comparisons: calcium ion release of day 7

(I) contaminate	(J) contaminate	Mean Difference (I-J)	Std. Error	Sig.[a]	95% Confidence Interval for Difference[a]	
					Lower Bound	Upper Bound
Non-blood	blood	.605	13.962	.966	-28.211	29.421
blood	Non-blood	-.605	13.962	.966	-29.421	28.211

Based on estimated marginal means

a. Adjustment for multiple comparisons: Bonferroni.

Table 31: Descriptive Statistics: calcium ion release of day 14

materials	contaminate	Mean	Std. Deviation	N
WMTA	Non-blood	60.69800	39.139321	5
	blood	72.39000	57.724346	5
	Total	66.54400	46.901437	10
Biodentine	Non-blood	159.73200	54.096138	5
	blood	160.73200	52.761531	5
	Total	160.23200	50.379874	10
TRRM	Non-blood	124.97400	33.873668	5
	blood	121.74000	32.593680	5
	Total	123.35700	31.385135	10
Total	Non-blood	115.13467	58.351302	15
	blood	118.28733	58.744658	15
	Total	116.71100	57.552338	30

Table 32: Tests of Between-Subjects Effects: calcium ion release of day 14

Source	Type III Sum of Squares	df	Mean Square	F	Sig.
Corrected Model	44920.151[a]	5	8984.030	4.217	.007
Intercept	408643.726	1	408643.726	191.793	.000
materials	44549.746	2	22274.873	10.454	.001
contaminate	74.545	1	74.545	.035	.853
materials * contaminate	295.859	2	147.930	.069	.933
Error	51135.725	24	2130.655		
Total	504699.601	30			
Corrected Total	96055.875	29			

a. R Squared = .468 (Adjusted R Squared = .357)

Table 33: Pairwise Comparisons: calcium ion release of day 14

(I) materials	(J) materials	Mean Difference (I-J)	Std. Error	Sig.[b]	95% Confidence Interval for Difference[b]	
					Lower Bound	Upper Bound
WMTA	Biodentine	-93.688*	20.643	.000	-146.816	-40.560
	TRRM	-56.813*	20.643	.033	-109.941	-3.685
Biodentine	WMTA	93.688*	20.643	.000	40.560	146.816
	TRRM	36.875	20.643	.260	-16.253	90.003
TRRM	WMTA	56.813*	20.643	.033	3.685	109.941
	Biodentine	-36.875	20.643	.260	-90.003	16.253

Based on estimated marginal means

*. The mean difference is significant at the .05 level.

b. Adjustment for multiple comparisons: Bonferroni.

Table 34: Pairwise Comparisons: calcium ion release of day 14

(I) contaminate	(J) contaminate	Mean Difference (I-J)	Std. Error	Sig.[a]	95% Confidence Interval for Difference[a]	
					Lower Bound	Upper Bound
Non-blood	blood	-3.153	16.855	.853	-37.939	31.634
blood	Non-blood	3.153	16.855	.853	-31.634	37.939

Based on estimated marginal means

a. Adjustment for multiple comparisons: Bonferroni.

Table 35: Descriptive Statistics: calcium ion release of day 28

materials	contaminate	Mean	Std. Deviation	N
WMTA	Non-blood	38.82000	22.696696	5
	blood	39.96200	8.127688	5
	Total	39.39100	16.083317	10
Biodentine	Non-blood	114.83600	23.290674	5
	blood	113.30400	32.159261	5
	Total	114.07000	26.483877	10
TRRM	Non-blood	83.22000	18.100927	5
	blood	65.82400	18.557627	5
	Total	74.52200	19.563766	10
Total	Non-blood	78.95867	37.912709	15
	blood	73.03000	37.431578	15
	Total	75.99433	37.140260	30

Table 36: Tests of Between-Subjects Effects: calcium ion release of day 28

Source	Type III Sum of Squares	df	Mean Square	F	Sig.
Corrected Model	28682.962[a]	5	5736.592	12.163	.000
Intercept	173254.161	1	173254.161	367.336	.000
materials	27917.282	2	13958.641	29.595	.000
contaminate	263.618	1	263.618	.559	.462
materials * contaminate	502.062	2	251.031	.532	.594
Error	11319.608	24	471.650		
Total	213256.730	30			
Corrected Total	40002.570	29			

a. R Squared = .717 (Adjusted R Squared = .658)

Table 37: Pairwise Comparisons: calcium ion release of day 28

(I) materials	(J) materials	Mean Difference (I-J)	Std. Error	Sig.[b]	95% Confidence Interval for Difference[b]	
					Lower Bound	Upper Bound
WMTA	Biodentine	-74.679*	9.712	.000	-99.675	-49.683
	TRRM	-35.131*	9.712	.004	-60.127	-10.135
Biodentine	WMTA	74.679*	9.712	.000	49.683	99.675
	TRRM	39.548*	9.712	.001	14.552	64.544
TRRM	WMTA	35.131*	9.712	.004	10.135	60.127
	Biodentine	-39.548*	9.712	.001	-64.544	-14.552

Based on estimated marginal means

*. The mean difference is significant at the .05 level.

b. Adjustment for multiple comparisons: Bonferroni.

Table 38: Pairwise Comparisons: calcium ion release of day 28

(I) contaminate	(J) contaminate	Mean Difference (I-J)	Std. Error	Sig.[a]	95% Confidence Interval for Difference[a]	
					Lower Bound	Upper Bound
Non-blood	blood	5.929	7.930	.462	-10.438	22.296
blood	Non-blood	-5.929	7.930	.462	-22.296	10.438

Based on estimated marginal means

a. Adjustment for multiple comparisons: Bonferroni.

APPENDIX C

Silicon ion release

Table 39: Descriptive Statistics: silicon ion release of day 1

materials	contaminate	Mean	Std. Deviation	N
MTA	no blood	1.21860	.128683	5
	blood	.87900	.136079	5
	Total	1.04880	.218232	10
Biodentine	no blood	.80060	.101095	5
	blood	.41720	.142224	5
	Total	.60890	.233162	10
TRRM	no blood	.78480	.075761	5
	blood	.48460	.099427	5
	Total	.63470	.178824	10
Total	no blood	.93467	.229181	15
	blood	.59360	.241540	15
	Total	.76413	.289147	30

Table 40: Tests of Between-Subjects Effects: silicon ion release of day 1

Source	Type III Sum of Squares	df	Mean Square	F	Sig.
Corrected Model	2.100[a]	5	.420	31.053	.000
Intercept	17.517	1	17.517	1295.152	.000
materials	1.219	2	.609	45.059	.000
contaminate	.872	1	.872	64.506	.000
materials * contaminate	.009	2	.004	.320	.729
Error	.325	24	.014		
Total	19.942	30			
Corrected Total	2.425	29			

a. R Squared = .866 (Adjusted R Squared = .838)

Table 41: Pairwise Comparisons: silicon ion release of day 1

(I) materials	(J) materials	Mean Difference (I-J)	Std. Error	Sig.[b]	95% Confidence Interval for Difference[b]	
					Lower Bound	Upper Bound
MTA	Biodentine	.440*	.052	.000	.306	.574
	TRRM	.414*	.052	.000	.280	.548
Biodentine	MTA	-.440*	.052	.000	-.574	-.306
	TRRM	-.026	.052	1.000	-.160	.108
TRRM	MTA	-.414*	.052	.000	-.548	-.280
	Biodentine	.026	.052	1.000	-.108	.160

Based on estimated marginal means

*. The mean difference is significant at the .05 level.

b. Adjustment for multiple comparisons: Bonferroni.

Table 42: Pairwise Comparisons: silicon ion release of day 1

(I) contaminate	(J) contaminate	Mean Difference (I-J)	Std. Error	Sig.[b]	95% Confidence Interval for Difference[b]	
					Lower Bound	Upper Bound
no blood	blood	.341*	.042	.000	.253	.429
blood	no blood	-.341*	.042	.000	-.429	-.253

Based on estimated marginal means

*. The mean difference is significant at the .05 level.

b. Adjustment for multiple comparisons: Bonferroni.

Table 43: Descriptive Statistics: silicon ion release of day 7

materials	contaminate	Mean	Std. Deviation	N
MTA	no blood	1.64860	.182526	5
	blood	1.11860	.208674	5
	Total	1.38360	.334945	10
Biodentine	no blood	.94120	.130080	5
	blood	.64460	.136256	5
	Total	.79290	.200520	10
TRRM	no blood	.96020	.123163	5
	blood	.57380	.143233	5
	Total	.76700	.239444	10
Total	no blood	1.18333	.367042	15
	blood	.77900	.293744	15
	Total	.98117	.385970	30

Table 44: Tests of Between-Subjects Effects: silicon ion release of day 7

Source	Type III Sum of Squares	df	Mean Square	F	Sig.
Corrected Model	3.728[a]	5	.746	30.221	.000
Intercept	28.881	1	28.881	1170.584	.000
materials	2.433	2	1.216	49.300	.000
contaminate	1.226	1	1.226	49.698	.000
materials * contaminate	.069	2	.035	1.404	.265
Error	.592	24	.025		
Total	33.201	30			
Corrected Total	4.320	29			

a. R Squared = .863 (Adjusted R Squared = .834)

Table 45: Pairwise Comparisons: silicon ion release of day 7

(I) materials	(J) materials	Mean Difference (I-J)	Std. Error	Sig.[b]	95% Confidence Interval for Difference[b]	
					Lower Bound	Upper Bound
MTA	Biodentine	.591*	.070	.000	.410	.771
	TRRM	.617*	.070	.000	.436	.797
Biodentine	MTA	-.591*	.070	.000	-.771	-.410
	TRRM	.026	.070	1.000	-.155	.207
TRRM	MTA	-.617*	.070	.000	-.797	-.436
	Biodentine	-.026	.070	1.000	-.207	.155

Based on estimated marginal means

*. The mean difference is significant at the .05 level.

b. Adjustment for multiple comparisons: Bonferroni.

Table 46: Pairwise Comparisons: silicon ion release of day 7

(I) contaminate	(J) contaminate	Mean Difference (I-J)	Std. Error	Sig.[b]	95% Confidence Interval for Difference[b]	
					Lower Bound	Upper Bound
no blood	blood	.404*	.057	.000	.286	.523
blood	no blood	-.404*	.057	.000	-.523	-.286

Based on estimated marginal means

*. The mean difference is significant at the .05 level.

b. Adjustment for multiple comparisons: Bonferroni.

Table 47: Descriptive Statistics: silicon ion release of day 14

materials	contaminate	Mean	Std. Deviation	N
MTA	no blood	1.40840	.204542	5
	blood	.76840	.180313	5
	Total	1.08840	.383174	10
Biodentine	no blood	.83320	.133061	5
	blood	.44560	.086495	5
	Total	.63940	.230056	10
TRRM	no blood	.76260	.112021	5
	blood	.49120	.048142	5
	Total	.62690	.164523	10
Total	no blood	1.00140	.332006	15
	blood	.56840	.184090	15
	Total	.78490	.343602	30

Table 48: Tests of Between-Subjects Effects: silicon ion release of day 14

Source	Type III Sum of Squares	df	Mean Square	F	Sig.
Corrected Model	2.966[a]	5	.593	31.113	.000
Intercept	18.482	1	18.482	969.312	.000
materials	1.382	2	.691	36.252	.000
contaminate	1.406	1	1.406	73.748	.000
materials * contaminate	.178	2	.089	4.656	.020
Error	.458	24	.019		
Total	21.906	30			
Corrected Total	3.424	29			

a. R Squared = .866 (Adjusted R Squared = .838)

Table 49: Pairwise Comparisons: silicon ion release of day 14

(I) materials	(J) materials	Mean Difference (I-J)	Std. Error	Sig.[b]	95% Confidence Interval for Difference[b]	
					Lower Bound	Upper Bound
MTA	Biodentine	.449*	.062	.000	.290	.608
	TRRM	.461*	.062	.000	.303	.620
Biodentine	MTA	-.449*	.062	.000	-.608	-.290
	TRRM	.012	.062	1.000	-.146	.171
TRRM	MTA	-.461*	.062	.000	-.620	-.303
	Biodentine	-.012	.062	1.000	-.171	.146

Based on estimated marginal means

*. The mean difference is significant at the .05 level.

b. Adjustment for multiple comparisons: Bonferroni.

Table 50: Pairwise Comparisons: silicon ion release of day 14

(I) contaminate	(J) contaminate	Mean Difference (I-J)	Std. Error	Sig.[b]	95% Confidence Interval for Difference[b]	
					Lower Bound	Upper Bound
no blood	blood	.433*	.050	.000	.329	.537
blood	no blood	-.433*	.050	.000	-.537	-.329

Based on estimated marginal means

*. The mean difference is significant at the .05 level.

b. Adjustment for multiple comparisons: Bonferroni.

Table 51: Descriptive Statistics: silicon ion release of day 28

materials	contaminate	Mean	Std. Deviation	N
MTA	no blood	1.49920	.258976	5
	blood	.85960	.154029	5
	Total	1.17940	.392413	10
Biodentine	no blood	.79500	.147948	5
	blood	.40140	.052434	5
	Total	.59820	.232344	10
TRRM	no blood	.70920	.121798	5
	blood	.41980	.084916	5
	Total	.56450	.181831	10
Total	no blood	1.00113	.404802	15
	blood	.56027	.240177	15
	Total	.78070	.396511	30

Table 52: Tests of Between-Subjects Effects: silicon ion release of day 28

Source	Type III Sum of Squares	df	Mean Square	F	Sig.
Corrected Model	4.010[a]	5	.802	34.998	.000
Intercept	18.285	1	18.285	798.016	.000
materials	2.390	2	1.195	52.157	.000
contaminate	1.458	1	1.458	63.621	.000
materials * contaminate	.162	2	.081	3.528	.045
Error	.550	24	.023		
Total	22.844	30			
Corrected Total	4.559	29			

a. R Squared = .879 (Adjusted R Squared = .854)

Table 53: Pairwise Comparisons: silicon ion release of day 28

(I) materials	(J) materials	Mean Difference (I-J)	Std. Error	Sig.[b]	95% Confidence Interval for Difference[b]	
					Lower Bound	Upper Bound
MTA	Biodentine	.581*	.068	.000	.407	.755
	TRRM	.615*	.068	.000	.441	.789
Biodentine	MTA	-.581*	.068	.000	-.755	-.407
	TRRM	.034	.068	1.000	-.141	.208
TRRM	MTA	-.615*	.068	.000	-.789	-.441
	Biodentine	-.034	.068	1.000	-.208	.141

Based on estimated marginal means

*. The mean difference is significant at the .05 level.

b. Adjustment for multiple comparisons: Bonferroni.

Table 54: Pairwise Comparisons: silicon ion release of day 28

(I) contaminate	(J) contaminate	Mean Difference (I-J)	Std. Error	Sig.[b]	95% Confidence Interval for Difference[b]	
					Lower Bound	Upper Bound
no blood	blood	.441*	.055	.000	.327	.555
blood	no blood	-.441*	.055	.000	-.555	-.327

Based on estimated marginal means

*. The mean difference is significant at the .05 level.

b. Adjustment for multiple comparisons: Bonferroni.

REFERENCES

1. Ford TR, Torabinejad M, McKendry DJ, Hong CU, Kariyawasam SP. Use of mineral trioxide aggregate for repair of furcal perforations. Oral Surg Oral Med Oral Pathol Oral Radiol Endod. 1995;79(6):756-63.

2. Fuss Z, Trope M. Root perforations: classification and treatment choices based on prognostic factors. Endod Dent Traumatol. 1996;12(6):255-64.

3. Ma J, Shen Y, Stojicic S, Haapasalo M. Biocompatibility of two novel root repair materials. J Endod. 2011;37(6):793-8.

4. Camilleri J, Pitt Ford TR. Mineral trioxide aggregate: a review of the constituents and biological properties of the material. Int Endod J. 2006;39(10):747-54.

5. Reyes-Carmona JF, Felippe MS, Felippe WT. Biomineralization ability and interaction of mineral trioxide aggregate and white portland cement with dentin in a phosphate-containing fluid. J Endod. 2009;35(5):731-6.

6. Zhu Q, Haglund R, Safavi KE, Spangberg LS. Adhesion of human osteoblasts on root-end filling materials. J Endod. 2000;26(7):404-6.

7. Torabinejad M, Parirokh M. Mineral trioxide aggregate: a comprehensive literature review--part II: leakage and biocompatibility investigations. J Endod. 2010;36(2):190-202.

8. Sarkar NK, Caicedo R, Ritwik P, Moiseyeva R, Kawashima I. Physicochemical basis of the biologic properties of mineral trioxide aggregate. J Endod. 2005;31(2):97-100.

9. Bozeman TB, Lemon RR, Eleazer PD. Elemental analysis of crystal precipitate from gray and white MTA. J Endod. 2006;32(5):425-8.

10. Tay FR, Pashley DH, Rueggeberg FA, Loushine RJ, Weller RN. Calcium phosphate phase transformation produced by the interaction of the portland cement component of white mineral trioxide aggregate with a phosphate-containing fluid. J Endod. 2007;33(11):1347-51.

11. Gandolfi MG, Taddei P, Tinti A, Prati C. Apatite-forming ability (bioactivity) of ProRoot MTA. Int Endod J. 2010;43(10):917-29.

12. Han L, Okiji T, Okawa S. Morphological and chemical analysis of different

precipitates on mineral trioxide aggregate immersed in different fluids. Dent Mater J. 2010;29(5):512-7.

13. Kokubo T. Bioactive glass ceramics: properties and applications. Biomaterials. 1991;12(2):155-63.

14. Kasuga T. Bioactive calcium pyrophosphate glasses and glass-ceramics. Acta Biomater. 2005;1(1):55-64.

15. Han L, Okiji T. Uptake of calcium and silicon released from calcium silicate-based endodontic materials into root canal dentine. Int Endod J. 2011;44(12):1081-7.

16. Torabinejad M, Hong CU, McDonald F, Pitt Ford TR. Physical and chemical properties of a new root-end filling material. J Endod. 1995;21(7):349-53.

17. Dammaschke T, Gerth HU, Zuchner H, Schafer E. Chemical and physical surface and bulk material characterization of white ProRoot MTA and two Portland cements. Dent Mater. 2005;21(8):731-8.

18. Lenherr P, Allgayer N, Weiger R, Filippi A, Attin T, Krastl G. Tooth discoloration induced by endodontic materials: a laboratory study. Int Endod J. 2012;45(10):942-9.

19. Felman D, Parashos P. Coronal tooth discoloration and white mineral trioxide aggregate. J Endod. 2013;39(4):484-7.

20. Nekoofar MH, Davies TE, Stone D, Basturk FB, Dummer PM. Microstructure and chemical analysis of blood-contaminated mineral trioxide aggregate. Int Endod J. 2011;44(11):1011-8.

21. Goldberg M, Pradelle-Plasse N, Tran X, Colon P, Laurent P, Aubut V. Emerging trends in (bio) material researches. Biocompatibility or cytotoxic effects of dental composites Oxford, UK: Coxmoor Publishing. 2009:181-203.

22. Laurent P, Camps J, About I. Biodentine(TM) induces TGF-beta1 release from human pulp cells and early dental pulp mineralization. Int Endod J. 2012;45(5):439-48.

23. Zanini M, Sautier JM, Berdal A, Simon S. Biodentine induces immortalized murine pulp cell differentiation into odontoblast-like cells and stimulates biomineralization. J Endod. 2012;38(9):1220-6.

24. Loushine BA, Bryan TE, Looney SW, Gillen BM, Loushine RJ, Weller RN, et al.

Setting properties and cytotoxicity evaluation of a premixed bioceramic root canal sealer. J Endod. 2011;37(5):673-7.

25. Damas BA, Wheater MA, Bringas JS, Hoen MM. Cytotoxicity comparison of mineral trioxide aggregates and EndoSequence bioceramic root repair materials. J Endod. 2011;37(3):372-5.

26. Hirschman WR, Wheater MA, Bringas JS, Hoen MM. Cytotoxicity comparison of three current direct pulp-capping agents with a new bioceramic root repair putty. J Endod. 2012;38(3):385-8.

27. Shokouhinejad N, Nekoofar MH, Razmi H, Sajadi S, Davies TE, Saghiri MA, et al. Bioactivity of EndoSequence root repair material and bioaggregate. Int Endod J. 2012;45(12):1127-34.

28. Gartner AH, Dorn SO. Advances in endodontic surgery. Dent Clin North Am. 1992;36(2):357-78.

29. Lemon RR. Nonsurgical repair of perforation defects. Internal matrix concept. Dent Clin North Am. 1992;36(2):439-57.

30. Torabinejad M, Higa RK, McKendry DJ, Pitt Ford TR. Dye leakage of four root end filling materials: effects of blood contamination. J Endod. 1994;20(4):159-63.

31. Montellano AM, Schwartz SA, Beeson TJ. Contamination of tooth-colored mineral trioxide aggregate used as a root-end filling material: a bacterial leakage study. J Endod. 2006;32(5):452-5.

32. Vanderweele RA, Schwartz SA, Beeson TJ. Effect of blood contamination on retention characteristics of MTA when mixed with different liquids. J Endod. 2006;32(5):421-4.

33. Arens DE, Torabinejad M. Repair of furcal perforations with mineral trioxide aggregate: two case reports. Oral Surg Oral Med Oral Pathol Oral Radiol Endod. 1996;82(1):84-8.

34. Sluyk SR, Moon PC, Hartwell GR. Evaluation of setting properties and retention characteristics of mineral trioxide aggregate when used as a furcation perforation repair material. J Endod. 1998;24(11):768-71.

35. Al-Daafas A, Al-Nazhan S. Histological evaluation of contaminated furcal perforation in dogs' teeth repaired by MTA with or without internal matrix. Oral Surg Oral Med Oral Pathol Oral Radiol Endod. 2007;103(3):e92-9.

36. Glickman G, Mickel A, Levin L, Fouad A, Johnson W. Glossary of endodontic terms. Chicago Am Assoc Endodontists. 2003:1-51.

37. Farzaneh M, Abitbol S, Friedman S. Treatment outcome in endodontics: the Toronto study. Phases I and II: Orthograde retreatment. J Endod. 2004;30(9):627-33.

38. Seltzer S, Sinai I, August D. Periodontal effects of root perforations before and during endodontic procedures. J Dent Res. 1970;49(2):332-9.

39. ElDeeb ME, ElDeeb M, Tabibi A, Jensen JR. An evaluation of the use of amalgam, Cavit, and calcium hydroxide in the repair of furcation perforations. J Endod. 1982;8(10):459-66.

40. Alhadainy HA, Himel VT. Evaluation of the sealing ability of amalgam, Cavit, and glass ionomer cement in the repair of furcation perforations. Oral Surg Oral Med Oral Pathol. 1993;75(3):362-6.

41. Harris WE. A simplified method of treatment for endodontic perforations. J Endod. 1976;2(5):126-34.

42. Breault LG, Fowler EB, Primack PD. Endodontic perforation repair with resin-ionomer: a case report. J Contemp Dent Pract. 2000;1(4):48-59.

43. Rud J, Rud V, Munksgaard EC. Retrograde sealing of accidental root perforations with dentin-bonded composite resin. J Endod. 1998;24(10):671-7.

44. Alhadainy HA, Himel VT. Comparative study of the sealing ability of light-cured versus chemically cured materials placed into furcation perforations. Oral Surg Oral Med Oral Pathol. 1993;76(3):338-42.

45. Wang Z. Bioceramic materials in endodontics. Endodontic Topics. 2015;32(1):3-30.

46. Santos AD, Araujo EB, Yukimitu K, Barbosa JC, Moraes JC. Setting time and thermal expansion of two endodontic cements. Oral Surg Oral Med Oral Pathol Oral Radiol Endod. 2008;106(3):e77-9.

47. Okabe T, Sakamoto M, Takeuchi H, Matsushima K. Effects of pH on mineralization ability of human dental pulp cells. J Endod. 2006;32(3):198-201.

48. Holland R, de Souza V, Nery MJ, Otoboni Filho JA, Bernabe PF, Dezan Junior E. Reaction of rat connective tissue to implanted dentin tubes filled with mineral trioxide aggregate or calcium hydroxide. J Endod. 1999;25(3):161-6.

49. Candeiro GT, Correia FC, Duarte MA, Ribeiro-Siqueira DC, Gavini G. Evaluation of radiopacity, pH, release of calcium ions, and flow of a bioceramic root canal sealer. J Endod. 2012;38(6):842-5.

50. Silva EJ, Rosa TP, Herrera DR, Jacinto RC, Gomes BP, Zaia AA. Evaluation of cytotoxicity and physicochemical properties of calcium silicate-based endodontic sealer MTA Fillapex. J Endod. 2013;39(2):274-7.

51. Fridland M, Rosado R. Mineral trioxide aggregate (MTA) solubility and porosity with different water-to-powder ratios. J Endod. 2003;29(12):814-7.

52. Jasiczak J, Zielinski K. Effect of protein additive on properties of mortar. Cement and Concrete Composites. 2006;28(5):451-7.

53. Mehta PK, Monteiro PJM. Concrete : microstructure, properties, and materials. 3rd ed. ed. New York ; London: McGraw-Hill; 2006.

54. Namazikhah MS, Nekoofar MH, Sheykhrezae MS, Salariyeh S, Hayes SJ, Bryant ST, et al. The effect of pH on surface hardness and microstructure of mineral trioxide aggregate. Int Endod J. 2008;41(2):108-16.

55. Asgary S, Parirokh M, Eghbal MJ, Brink F. Chemical differences between white and gray mineral trioxide aggregate. J Endod. 2005;31(2):101-3.

56. Song JS, Mante FK, Romanow WJ, Kim S. Chemical analysis of powder and set forms of Portland cement, gray ProRoot MTA, white ProRoot MTA, and gray MTA-Angelus. Oral Surg Oral Med Oral Pathol Oral Radiol Endod. 2006;102(6):809-15.

57. Saghiri MA, Gutmann JL, Orangi J, Asatourian A, Sheibani N. Radiopacifier particle size impacts the physical properties of tricalcium silicate-based cements. J Endod. 2015;41(2):225-30.

58. Camilleri J. Composition and Setting Reaction. In: Camilleri J, editor. Mineral

Trioxide Aggregate in Dentistry: From Preparation to Application. Berlin, Heidelberg: Springer Berlin Heidelberg; 2014. p. 19-36.

59. Camilleri J. Characterization of hydration products of mineral trioxide aggregate. Int Endod J. 2008;41(5):408-17.

60. Torabinejad M, Watson TF, Pitt Ford TR. Sealing ability of a mineral trioxide aggregate when used as a root end filling material. J Endod. 1993;19(12):591-5.

61. Gandolfi MG, Iacono F, Agee K, Siboni F, Tay F, Pashley DH, et al. Setting time and expansion in different soaking media of experimental accelerated calcium-silicate cements and ProRoot MTA. Oral Surg Oral Med Oral Pathol Oral Radiol Endod. 2009;108(6):e39-45.

62. Bortoluzzi EA, Broon NJ, Bramante CM, Felippe WT, Tanomaru Filho M, Esberard RM. The influence of calcium chloride on the setting time, solubility, disintegration, and pH of mineral trioxide aggregate and white Portland cement with a radiopacifier. J Endod. 2009;35(4):550-4.

63. Camilleri J, Montesin FE, Brady K, Sweeney R, Curtis RV, Ford TR. The constitution of mineral trioxide aggregate. Dent Mater. 2005;21(4):297-303.

64. Islam I, Chng HK, Yap AU. Comparison of the physical and mechanical properties of MTA and portland cement. J Endod. 2006;32(3):193-7.

65. Fridland M, Rosado R. MTA solubility: a long term study. J Endod. 2005;31(5):376-9.

66. Ozdemir HO, Ozcelik B, Karabucak B, Cehreli ZC. Calcium ion diffusion from mineral trioxide aggregate through simulated root resorption defects. Dent Traumatol. 2008;24(1):70-3.

67. Poggio C, Lombardini M, Alessandro C, Simonetta R. Solubility of root-end-filling materials: a comparative study. J Endod. 2007;33(9):1094-7.

68. Danesh G, Dammaschke T, Gerth HU, Zandbiglari T, Schafer E. A comparative study of selected properties of ProRoot mineral trioxide aggregate and two Portland cements. Int Endod J. 2006;39(3):213-9.

69. de Vasconcelos BC, Bernardes RA, Cruz SM, Duarte MA, Padilha Pde M,

Bernardineli N, et al. Evaluation of pH and calcium ion release of new root-end filling materials. Oral Surg Oral Med Oral Pathol Oral Radiol Endod. 2009;108(1):135-9.

70. Lee YL, Lee BS, Lin FH, Yun Lin A, Lan WH, Lin CP. Effects of physiological environments on the hydration behavior of mineral trioxide aggregate. Biomaterials. 2004;25(5):787-93.

71. Tingey MC, Bush P, Levine MS. Analysis of mineral trioxide aggregate surface when set in the presence of fetal bovine serum. J Endod. 2008;34(1):45-9.

72. Kang JS, Rhim EM, Huh SY, Ahn SJ, Kim DS, Kim SY, et al. The effects of humidity and serum on the surface microhardness and morphology of five retrograde filling materials. Scanning. 2012;34(4):207-14.

73. Kim Y, Kim S, Shin YS, Jung IY, Lee SJ. Failure of setting of mineral trioxide aggregate in the presence of fetal bovine serum and its prevention. J Endod. 2012;38(4):536-40.

74. Grech L, Mallia B, Camilleri J. Investigation of the physical properties of tricalcium silicate cement-based root-end filling materials. Dent Mater. 2013;29(2):e20-8.

75. Camilleri J, Sorrentino F, Damidot D. Investigation of the hydration and bioactivity of radiopacified tricalcium silicate cement, Biodentine and MTA Angelus. Dent Mater. 2013;29(5):580-93.

76. Camilleri J, Kralj P, Veber M, Sinagra E. Characterization and analyses of acid-extractable and leached trace elements in dental cements. Int Endod J. 2012;45(8):737-43.

77. Biodentine-Septodont R. Department: Biodentine. Active biosilicate technology. Scientific file.

78. Camilleri J. Investigation of Biodentine as dentine replacement material. J Dent. 2013;41(7):600-10.

79. Khan SIR, Ramachandran A, Deepalakshmi M, Kumar KS. Evaluation of pH and calcium ion release of mineral trioxide aggregate and a new root-end filling material. EJ Dentistry. 2012;2:166-9.

80. Grech L, Mallia B, Camilleri J. Characterization of set Intermediate Restorative

Material, Biodentine, Bioaggregate and a prototype calcium silicate cement for use as root-end filling materials. Int Endod J. 2013;46(7):632-41.

81. Han L, Okiji T. Bioactivity evaluation of three calcium silicate-based endodontic materials. Int Endod J. 2013;46(9):808-14.

82. Hansen SW, Marshall JG, Sedgley CM. Comparison of intracanal EndoSequence Root Repair Material and ProRoot MTA to induce pH changes in simulated root resorption defects over 4 weeks in matched pairs of human teeth. J Endod. 2011;37(4):502-6.

83. Kayahan MB, Nekoofar MH, Kazandag M, Canpolat C, Malkondu O, Kaptan F, et al. Effect of acid-etching procedure on selected physical properties of mineral trioxide aggregate. Int Endod J. 2009;42(11):1004-14.

84. Nekoofar MH, Oloomi K, Sheykhrezae MS, Tabor R, Stone DF, Dummer PM. An evaluation of the effect of blood and human serum on the surface microhardness and surface microstructure of mineral trioxide aggregate. Int Endod J. 2010;43(10):849-58.

85. Nekoofar MH, Stone DF, Dummer PM. The effect of blood contamination on the compressive strength and surface microstructure of mineral trioxide aggregate. Int Endod J. 2010;43(9):782-91.

86. Remadnia A, Dheilly R, Laidoudi B, Quéneudec M. Use of animal proteins as foaming agent in cementitious concrete composites manufactured with recycled PET aggregates. Construction and Building Materials. 2009;23(10):3118-23.

87. Hewlett P. Lea's chemistry of cement and concrete: Butterworth-Heinemann; 2003.

88. Charland T, Hartwell GR, Hirschberg C, Patel R. An evaluation of setting time of mineral trioxide aggregate and EndoSequence root repair material in the presence of human blood and minimal essential media. J Endod. 2013;39(8):1071-2.

89. Alhodiry W, Lyons MF, Chadwick RG. Effect of saliva and blood contamination on the bi-axial flexural strength and setting time of two calcium-silicate based cements: Portland cement and biodentine. Eur J Prosthodont Restor Dent. 2014;22(1):20-3.

90. Gandolfi MG, Siboni F, Primus CM, Prati C. Ion release, porosity, solubility, and bioactivity of MTA Plus tricalcium silicate. J Endod. 2014;40(10):1632-7.

91. Gandolfi MG, Taddei P, Modena E, Siboni F, Prati C. Biointeractivity-related versus

chemi/physisorption-related apatite precursor-forming ability of current root end filling materials. J Biomed Mater Res B Appl Biomater. 2013;101(7):1107-23.

92. Ding S-J, Shie M-Y, Wang C-Y. Novel fast-setting calcium silicate bone cements with high bioactivity and enhanced osteogenesis in vitro. Journal of Materials Chemistry. 2009;19(8):1183-90.

93. Porter AE, Botelho CM, Lopes MA, Santos JD, Best SM, Bonfield W. Ultrastructural comparison of dissolution and apatite precipitation on hydroxyapatite and silicon-substituted hydroxyapatite in vitro and in vivo. Journal of Biomedical Materials Research Part A. 2004;69(4):670-9.

94. Porter AE. Nanoscale characterization of the interface between bone and hydroxyapatite implants and the effect of silicon on bone apposition. Micron. 2006;37(8):681-8.

95. Johnson BR. Considerations in the selection of a root-end filling material. Oral Surg Oral Med Oral Pathol Oral Radiol Endod. 1999;87(4):398-404.

96. Kokubo T, Takadama H. How useful is SBF in predicting in vivo bone bioactivity? Biomaterials. 2006;27(15):2907-15.

97. Gandolfi MG, Ciapetti G, Taddei P, Perut F, Tinti A, Cardoso MV, et al. Apatite formation on bioactive calcium-silicate cements for dentistry affects surface topography and human marrow stromal cells proliferation. Dent Mater. 2010;26(10):974-92.

98. Holland R, de Souza V, Nery MJ, Faraco Junior IM, Bernabe PF, Otoboni Filho JA, et al. Reaction of rat connective tissue to implanted dentin tube filled with mineral trioxide aggregate, Portland cement or calcium hydroxide. Braz Dent J. 2001;12(1):3-8.

99. Yang Q, Troczynski T, Liu DM. Influence of apatite seeds on the synthesis of calcium phosphate cement. Biomaterials. 2002;23(13):2751-60.

100. Zhang W, Li Z, Peng B. Assessment of a new root canal sealer's apical sealing ability. Oral Surg Oral Med Oral Pathol Oral Radiol Endod. 2009;107(6):e79-82.

101. Linsuwanont P. MTA apexification combined with conventional root canal retreatment. Aust Endod J. 2003;29(1):45-9.

102. Belio-Reyes IA, Bucio L, Cruz-Chavez E. Phase composition of ProRoot mineral

trioxide aggregate by X-ray powder diffraction. J Endod. 2009;35(6):875-8.

103. Camilleri J. Evaluation of the effect of intrinsic material properties and ambient conditions on the dimensional stability of white mineral trioxide aggregate and Portland cement. J Endod. 2011;37(2):239-45.

104. Neville A. Properties of Concrete (Fourth and Final ed.). Essex, England: Pearson Education. Longman Group; 2000.

105. Zhu L, Yang J, Zhang J, Lei D, Xiao L, Cheng X, et al. In vitro and in vivo evaluation of a nanoparticulate bioceramic paste for dental pulp repair. Acta Biomater. 2014;10(12):5156-68.

106. Lloyd GE. Atomic number and crystallographic contrast images with the SEM: a review of backscattered electron techniques. Mineralogical Magazine. 1987;51(359):3-19.

107. Cole D, Shallenberger J, Novak S, Moore R, Edgell M, Smith S, et al. SiO 2 thickness determination by x-ray photoelectron spectroscopy, Auger electron spectroscopy, secondary ion mass spectrometry, Rutherford backscattering, transmission electron microscopy, and ellipsometry. Journal of Vacuum Science & Technology B: Microelectronics and Nanometer Structures Processing, Measurement, and Phenomena. 2000;18(1):440-4.

108. Camilleri J. Hydration mechanisms of mineral trioxide aggregate. Int Endod J. 2007;40(6):462-70.

109. Rietveld H. A profile refinement method for nuclear and magnetic structures. Journal of applied Crystallography. 1969;2(2):65-71.

110. Stutzman PE, Leigh S, editors. Compositional analysis of NIST reference material clinker 8486. PROCEEDINGS OF THE INTERNATIONAL CONFERENCE ON CEMENT MICROSCOPY; 2000: INTERNATIONAL CEMENT MICROSCOPY ASSOCIATION.

111. Charles B, Fredeen KJ. Concepts, instrumentation and techniques in inductively coupled plasma optical emission spectrometry. Perkin Elmer Corporation. 1997.

112. Guerreiro-Tanomaru JM, de Faria-Junior NB, Duarte MA, Ordinola-Zapata R, Graeff MS, Tanomaru-Filho M. Comparative analysis of Enterococcus faecalis biofilm formation on different substrates. J Endod. 2013;39(3):346-50.

113. Park JW, Hong SH, Kim JH, Lee SJ, Shin SJ. X-Ray diffraction analysis of white ProRoot MTA and Diadent BioAggregate. Oral Surg Oral Med Oral Pathol Oral Radiol Endod. 2010;109(1):155-8.

114. Wang L, Nancollas GH. Calcium orthophosphates: crystallization and dissolution. Chemical reviews. 2008;108(11):4628-69.

115. Porter AE, Botelho CM, Lopes MA, Santos JD, Best SM, Bonfield W. Ultrastructural comparison of dissolution and apatite precipitation on hydroxyapatite and silicon-substituted hydroxyapatite in vitro and in vivo. Journal of Biomedical Materials Research Part A: An Official Journal of The Society for Biomaterials, The Japanese Society for Biomaterials, and The Australian Society for Biomaterials and the Korean Society for Biomaterials. 2004;69(4):670-9.

116. Camilleri J. Mineral trioxide aggregate in dentistry: From preparation to application: Springer; 2014. 1-206 p.

117. Carlisle EM. Silicon: a possible factor in bone calcification. Science. 1970;167(3916):279-80.

118. Tian J, Qi W, Zhang Y, Glogauer M, Wang Y, Lai Z, et al. Bioaggregate Inhibits Osteoclast Differentiation, Fusion, and Bone Resorption In Vitro. J Endod. 2015;41(9):1500-6.

119. Saito T, Toyooka H, Ito S, Crenshaw MA. In vitro study of remineralization of dentin: effects of ions on mineral induction by decalcified dentin matrix. Caries Res. 2003;37(6):445-9.

120. Maeno S, Niki Y, Matsumoto H, Morioka H, Yatabe T, Funayama A, et al. The effect of calcium ion concentration on osteoblast viability, proliferation and differentiation in monolayer and 3D culture. Biomaterials. 2005;26(23):4847-55.

121. Bortoluzzi EA, Broon NJ, Duarte MAH, de Oliveira Demarchi ACC, Bramante CM. The use of a setting accelerator and its effect on pH and calcium ion release of mineral trioxide aggregate and white Portland cement. Journal of endodontics. 2006;32(12):1194-7.

122. Okabe T, Sakamoto M, Takeuchi H, Matsushima K. Effects of pH on mineralization

ability of human dental pulp cells. Journal of endodontics. 2006;32(3):198-201.

123. Holland R, Souza Vd, Nery MJ, Faraco Júnior IM, Bernabé PFE, Otoboni Filho JA, et al. Reaction of rat connective tissue to implanted dentin tubes filled with a white mineral trioxide aggregate. Brazilian Dental Journal. 2002:23-6.

124. Guo YJ, Du TF, Li HB, Shen Y, Mobuchon C, Hieawy A, et al. Physical properties and hydration behavior of a fast-setting bioceramic endodontic material. BMC Oral Health. 2016;16:23.

125. Zhou HM, Shen Y, Zheng W, Li L, Zheng YF, Haapasalo M. Physical properties of 5 root canal sealers. J Endod. 2013;39(10):1281-6.

126. Nekoofar MH, Davies T, Stone D, Basturk F, Dummer PMH. Microstructure and chemical analysis of blood-contaminated mineral trioxide aggregate. International endodontic journal. 2011;44(11):1011-8.

VITA